TECHNICAL REPORT
NATICK/TR-92/009

AD _____

SELECTION OF OPENING MODEL FOR PARACHUTE SCALING STUDIES

By
Eugene E. Niemi, Jr.

University of Lowell
Lowell, MA 01854

MARCH 1992

Final Report
January 1990 - June 1991

APPROVED FOR PUBLIC RELEASE;
DISTRIBUTION UNLIMITED

Prepared for
UNITED STATES ARMY NATICK
RESEARCH, DEVELOPMENT AND ENGINEERING CENTER
NATICK, MASSACHUSETTS 01760-5000

AERO-MECHANICAL ENGINEERING DIRECTORATE

DISCLAIMERS

The findings contained in this report are not to be construed as an official Department of the Army position unless so designated by other authorized documents.

Citation of trade names in this report does not constitute an official endorsement or approval of the use of such items.

DESTRUCTION NOTICE

For Classified Documents:

Follow the procedures in DoD 5200.22-M, Industrial Security Manual, Section II-19 or DoD 5200.1-R, Information Security Program Regulation, Chapter IX.

For Unclassified/Limited Distribution Documents:

Destroy by any method that prevents disclosure of contents or reconstruction of the document.

REPORT DOCUMENTATION PAGE

Form Approved
OMB No. 0704-0188

1. AGENCY USE ONLY (Leave blank)	2. REPORT DATE	3. REPORT TYPE AND DATES COVERED
	March 1992	FINAL January 1990 - June 1990

4. TITLE AND SUBTITLE

SELECTION OF OPENING MODEL FOR PARACHUTE SCALING STUDIES

5. FUNDING NUMBERS

IPA 05-5179

6. AUTHOR(S)

Eugene E. Niemi, Jr.

7. PERFORMING ORGANIZATION NAME(S) AND ADDRESS(ES)

University of Lowell
One University Ave.
Lowell, MA 01854

8. PERFORMING ORGANIZATION REPORT NUMBER

9. SPONSORING/MONITORING AGENCY NAME(S) AND ADDRESS(ES)

U.S. Army Natick RD&E Center
ATTN: STRNC-UE
Natick, MA 01760-5017

10. SPONSORING/MONITORING AGENCY REPORT NUMBER

NATICK/TR-92/009

11. SUPPLEMENTARY NOTES

12a. DISTRIBUTION/AVAILABILITY STATEMENT

Approved for public release; distribution unlimited

12b. DISTRIBUTION CODE

13. ABSTRACT *(Maximum 200 words)*

This report consists of a summary of work to program an existing parachute opening dynamics theory for use with research into the scaling laws governing relationships between model and full-scale parachutes during the opening phase. The theory forms a basis to which modifications can be made to predict the opening dynamics of small-scale models. The object is eventually to be able to predict canopy stiffness effects on opening behavior.

14. SUBJECT TERMS	15. NUMBER OF PAGES
COMPUTER PROGRAMS SCALING THEORY PARACHUTE CANOPIES OPENING DYNAMICS PARACHUTES SCALING MODELS PARACHUTE OPENING STIFFNESS FLAT CIRCULAR PARACHUTES AERODYNAMIC DECELERATORS	53
	16. PRICE CODE

17. SECURITY CLASSIFICATION OF REPORT	18. SECURITY CLASSIFICATION OF THIS PAGE	19. SECURITY CLASSIFICATION OF ABSTRACT	20. LIMITATION OF ABSTRACT
UNCLASSIFIED	UNCLASSIFIED	UNCLASSIFIED	

Table of Contents

List of Illustrations

Preface

This report was prepared by the University of Lowell as part of IPA Research Project No. 05-5179. The work described in this report was performed between January 1 and June 30, 1990.

The work accomplished under this contract was sponsored by the US Army Natick Research, Development and Engineering Center, Aero-Mechanical Engineering Directorate, Engineering Technology Division. Dr. Earl C. Steeves was the project supervisor.

List of Symbols

Symbol	Fortran Symbol	Explanation
c_f	CF	Elasticity constant of a top cord
C_{eff}	CEF	Effective porosity
C_D	CD	Resistance coefficient of the parachute, referred to the projected area
C_{DL}	CDL	Resistance coefficient of the payload
d	DS	Damping constant of a top cord
D_o	DO	Nominal diameter of the parachute
D_C	DC	Construction diameter of the parachute
D	D	Resistance of air of the parachute
D_L	DL	Resistance of air of the payload
D_z	DZ	Damping constant ($D_z = ndD_o/m_L v_s$)
F	F	Filling force
F_s	FS	Deployment shock force
Fr	FR	Froude number ($Fr = V_s^2/gD_o$)
Fz	FZ	Elasticity coefficient ($Fz = nc_f D_o^2/m_L v_s^2$)
g	G	Acceleration of gravity
h	H	Lateral length of the truncated cone
h_{st}	HST	Lateral length of the truncated cone in the stationary state
k_1	XK1	Contraction factor for the first filling phase
k_2	XK2	Contraction factor for the second filling phase
l	XL	Length of a top cord under load

List of Symbols (Continued)

Symbol	Fortran Symbol	Explanation
l_s	XLS	Length of a top cord without load
m_a	XMA	Apparent mass
m_C	XMC	Mass of the parachute canopy
m_L	XML	Mass of the payload
m_S	XMS	Mass of the parachute canopy including apparent mass
m_T	XMT	Total mass of the system
n	XN	Number of top cords
r	R	Radius of the sphere
r_{st}	RST	Radius of the sphere in the stationary state
R	RP	Radius of the payload
R_v	RV	Radius of the apex aperture
s	S	Distance between the assumed centers of mass of the payload and parachute
t	T	Time
t_f	TF	Filling time
u	U	Mean speed of air flowing out through the porous fabric
v_C,v_L	VC,VL	Velocity of the parachute canopy and of payload
v_{Ct},v_{Cn}	VCT,VCN	Velocity component of the parachute canopy in tangential and normal direction
v_s	VS	Velocity of the payload in the deployment shock

List of Symbols (Continued)

Symbol	Fortran Symbol	Explanation
V	V	Volume of air trapped in the canopy
V_{st}	VST	Volume of air trapped in the canopy in the stationary state
w_t	RW	Relative velocity of the canopy against the payload in tangential direction
W_L	WL	Weight of the payload
W_T	WT	Total weight
X	–	"Wrap-around length" of canopy in first filling phase
Z	Z	Altitude
α_c, α_L	–	Angle of attack of canopy and payload
β	B	Semi-apertural angle of the top cords
β_{st}	BST	Semi-apertural angle of the top cords at the time of first full inflation
θ	TH	Angle of pitch (angle between the horizontal and the parachute axis of symmetry)
κ	XK	Proportionality constant
ρ	RHO	Air density
ω	XOM	Angular velocity of the parachute axis of symmetry

List of Symbols (Concluded)

Subscripts	Explanation
o	Initial

Superscripts	Explanation
-	Non-dimensional
	Derivative with respect to time

SELECTION OF OPENING MODEL FOR PARACHUTE SCALING STUDIES

Introduction

The purpose of this ongoing research project has been to identify those scaling laws important in modeling parachute opening dynamics, and to determine scaling parameters that will provide relationships in canopy stiffness.

Reference [1] summarizes the work done on this project during the time period from December 15, 1988, to December 14, 1989. During this period, an improved scaling parameter was developed for determining stiffness effects on the opening behavior of flat circular parachute canopies. This scaling parameter, called the relative stiffness index, worked well for correlating opening time of flat circular parachutes, and gave fair correlation for predicting opening shock for these canopies; but more work needed to be done on the opening shock method. In addition, the relative stiffness index concept should also be extended to other parachute geometries. The concept is well enough advanced, however, to justify its incorporation in some manner into an opening dynamics theory.

In the present work, a theory was chosen and computer programmed as a basis for allowing introduction of the stiffness concept and to provide a basis for later correlation of the test data available at Natick to further validate the use of the relative stiffness index.

Brief review of available theories

A listing of some of the various opening dynamics theories can be found in [2-13]. A critical review of some of the opening dynamics theories can be found in [14]. The two theories that proved most useful for this study were those developed by Fu [12] and Lingard [13].

Fu developed a theory to predict parachute opening shock and time, using a minimum of experimental inputs based on as little test data as possible. Fu considered the payload and canopy as two point masses connected by a spring with damping. The canopy shape was represented as a truncated cone topped with a hemispherical cap. The apparent mass of the parachute was assumed to be proportional to the canopy volume. The canopy vent size and effective porosity of the canopy fabric were considered in the conservation of mass equations used to model canopy filling. Using Newton's Law, Conservation of Mass, and the appropriate geometric relations, the writer derived a system of nonlinear differential equations. Some of the results of this theory are presented in [1].

Lingard's analysis for predicting opening shock was considerably different from that of Fu but led to similar results. His method was intended to provide a relatively simple theory to let a designer perform trade-offs upon the effects on the peak load of parameters such as snatch velocity, suspended mass, parachute size, and altitude

and angle of deployment. The main assumptions made by Lingard were as follows:

a. The parachute inflates in a constant nondimensional opening time independent of snatch velocity and mass ratio.

b. For a given parachute design, there exists a unique force coefficient vs. nondimensional time function which is independent of snatch velocity or mass ratio.

These two assumptions were then used to extract empirical data from a small number of full-scale tests of a particular solid cloth parachute system. With these assumptions, Newton's Second Law was then used to develop a model that allowed calculation of force and velocity profiles during deployment. The effects of the above-mentioned variables on deployment could then be studied.

A comparison of results from Lingard's and Fu's methods is given in [1] and will not be repeated here. The comparison shows similar trends in results from the two totally different approaches and lends confidence to the results obtained. Because of assumption (a) used above, Lingard's method is not useful in predicting Froude number and mass ratio effects on opening *time*, but the time assumption itself agrees fairly well with the theoretical results obtained by Fu.

More complex opening dynamics theories are also available, some of them being briefly summarized in [15]. However, most of these are far too complex for general use and not amenable to a reasonable simulation of opening dynamics, especially when parametric studies need to be conducted for a wide range of variables. The following quote, taken from [16] aptly depicts the situation regarding many of these prediction methods:

> The difficulty in predicting the performance of a parachute lies in the complex interaction between the porous canopy and the surrounding flow field. The parachute inflation process involves the unsteady, viscous, compressible flow about a porous body that undergoes large shape changes. Moreover, this body is composed of nonlinear materials with complex strain, strain rate, and hysteresis properties. Thus it is not surprising that a rigorous analysis of the Navier-Stokes equations for the unsteady flow about an inflating parachute presents a formidable challenge to existing computational capabilities. A recent study at Sandia National Laboratories concluded that an axisymmetric flow field solution for a typical weapons parachute would require 3300 hours on a CDC 7600 computer or 330 hours on a CRAY system. Hence, there exists an urgent need for a dependable intermediate theory useful for parachute design.

Continued work on canopy stiffness scaling laws will be hampered if a reasonable theory is not available that can be modified in some fashion to simulate canopy stiffness. Hence, the theories were examined to select one most suitable for this task.

The theories of Lingard and Fu referenced earlier seem to provide a reasonable compromise in accuracy without being excessively unwieldy. However, proper verification of these parachute opening theories will eventually require a wide range of tests. The scatter in test data creates this need. Most of these tests would have to be conducted outside the practical range of mass ratios and Froude numbers normally used in real parachute applications.

Conversely, at Froude numbers on the order of four to six where opening shock loads are reasonable, extrapolation of the theories of Fu and Lingard show almost no effect of typical mass ratio changes on nondimensional opening force. For this reason further tests need to be conducted at high Froude numbers over a wide range of mass ratios, and the theories of Fu or Lingard must be used to calculate expected parachute behavior at lower Froude numbers than they present in their works.

Basis for final selection of theory

The theory selected for programming must ultimately be one that appears suitable for modification to simulate canopy stiffness effects, be relatively complete (not oversimplified), yet amenable to computer programming and calculations at reasonable cost. The theory developed by Fu appeared to be the best for this purpose, if canopy stiffness effects can eventually be simulated using various input values for initial semi-aperture angle, bo (see Fig. 1), or some similar means. Heinrich and Hektner's stiffness index [17] used the inverted hang test of the canopy and an experimental measurement of Dmax to represent canopy stiffness. The Dmax and stiffness index values should be reflected in the initial semi-apertural angle bo in some manner. Fu's theory also allows part of the areal density effect of the fabric to be reflected by making an input change to canopy mass. Some of the effect of canopy stiffness could be accounted for by an adjustment to suspension line elasticity input, but this does not duplicate the main effect of canopy stiffness.

Major assumptions in the theory

The complete details and assumptions used by Fu will not be given in this report. The reader is referred to [12] for this information. The major assumptions and the models used to simulate the parachute opening geometry will be summarized, however. The parachute opening is broken down into a "first filling phase," "second filling phase," and "transition phase." The assumptions are as follows:

a. *First filling phase.* During the first filling phase, the parachute geometry is assumed as shown in Fig. 1.

   1. The initial semi-apertural angle, bo, is assumed to be a constant during this phase, and is obtained empirically.

   2. The canopy shape starts off as a small hemisphere and fills until the distance, X, is equal to the constructed diameter of the parachute. This determines the end of the first filling phase.

   3. During the first filling phase, no porosity or vent flow is assumed.

   4. The inflow area at the mouth of the parachute is taken to be a fraction of the actual area, using an empirical "contraction factor," k_1. The canopy velocity is used for the inflow velocity.

   5. A constant parachute drag coefficient (typically 0.5) is assumed during phase 1, and the drag changes with changes in projected frontal area and canopy velocity.

   6. Each suspension line is represented by a spring and damper, allowing for line stretch and a relative velocity between canopy and payload.

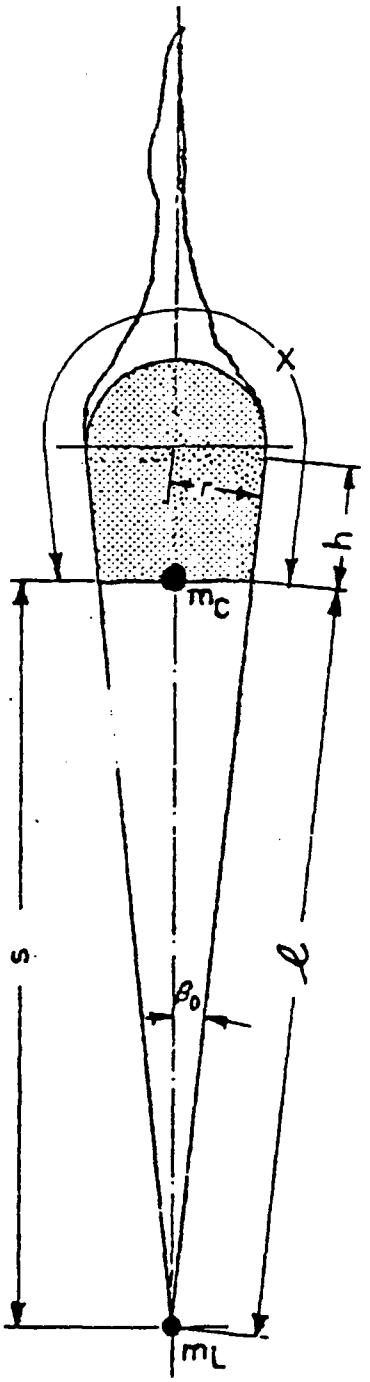

Fig. 1. Geometric Model of the Canopy for the First Filling Phase [12].

7. The initial suspension line stretch is determined from an input value for canopy snatch force.

8. In this phase, and all phases, the air is assumed incompressible.

As mentioned earlier, once the "wrap-around distance," X, equals the canopy constructed diameter, the first filling phase ends and the second filling phase begins.

b. *Second filling phase.* Fig. 2 shows the model used to represent the canopy during the second filling phase. The assumptions used to represent this portion of filling are as follows:

1. The shape of the canopy is assumed to be a truncated cone with a hemispherical cap. The wrap-around distance remains constant and equal to the constructed diameter, DC.

2. As air flows into the parachute mouth, the suspension line semi-apertural angle, β, increases, causing the hemispherical cap to grow larger in diameter while the sides of the truncated cone portion, h, decrease in length.

3. Conservation of mass applied to the inflow air governs the rate of canopy inflation. Air flow is allowed out through the vent and through the porous hemispherical portion of the canopy. An empirical contraction factor, k_2, different from k_1 in a.4., is used for this portion of the filling.

4. A new parachute drag coefficient (typically 1.3) is assumed during phase 2. Again, canopy drag changes with projected frontal area and canopy velocity.

5. Suspension lines are again represented by springs and dampers allowing for line stretch and a relative velocity between canopy and payload.

6. The second filling phase ends when the length of the sides of the truncated cone, h, has decreased to a value of $0.03\ D_o$. This is an empirical value obtained from motion pictures of parachute opening analyzed by Fu.

c. *Transition phase.* The transition phase is that phase that occurs between the end of the second filling phase and the time that steady state descent is reached. Fig. 3 shows the idealized geometry for the transition phase. The assumptions used in this phase are as follows:

1. The shape and size of the canopy remain constant at the steady state values h_{st}, $D_{c/2}$, r_{st}, and β_{st} as shown in Fig. 3. These values are the corresponding values that existed at the end of the second filling phase as defined by $h_{st} = h = 0.03\ D_o$.

2. The suspension lines are still represented by springs and dampers allowing for line stretch and relative velocity between canopy and payload. Thus, although the canopy shape remains unchanged, the semi-apertural angle, β, varies through a damped oscillation.

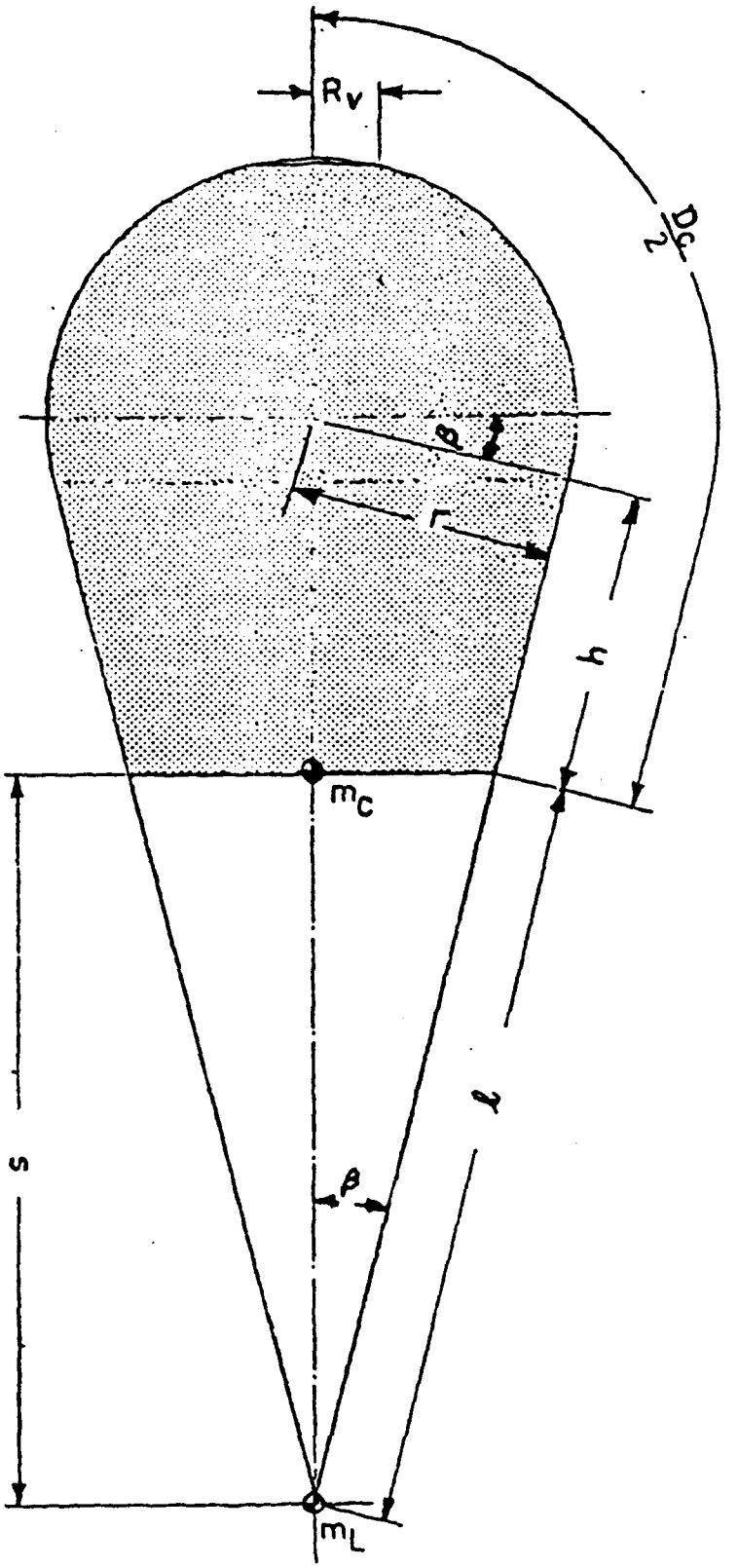

Fig. 2. Geometric Model of the Canopy for the Second Filling Phase [12].

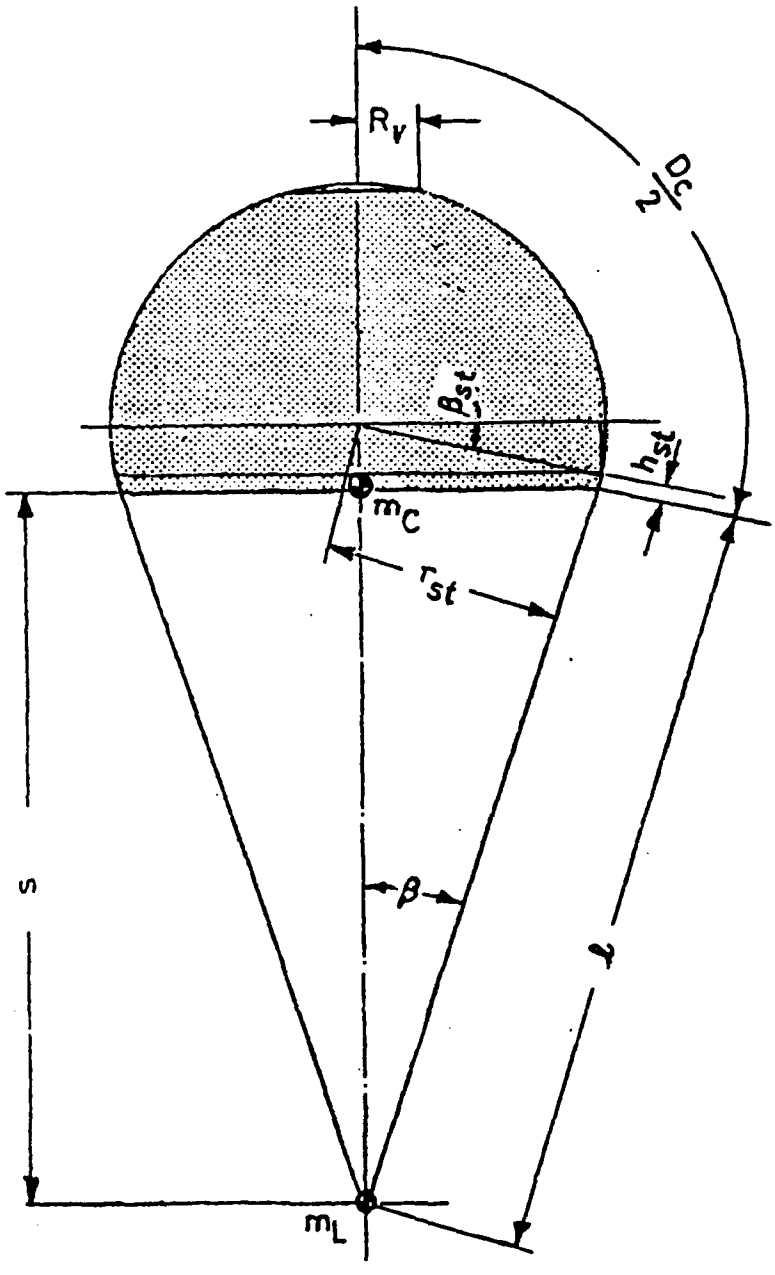

Fig. 3. Geometric Model of the Canopy for the Transition Phase [12].

3. Air flow is again accounted for through the vent and porous hemispherical portion of the canopy.

4. The drag coefficient is held constant at the value assumed for the second filling phase.

The transition phase ends when all geometric and trajectory parameters reach steady state values, i.e., the suspension line length, l, and semi-apertural angle, β, become constant, and the terminal velocity and vertical descent path are reached. Theoretically, this would occur asymptotically over a long period of time, but practically speaking, steady state values are approached closely in a period of several seconds. In any case, maximum filling force and opening time have already been calculated near the end of the second filling phase in most situations.

Fig. 4 is a simplified illustration of the velocity and acceleration components for the combined canopy and payload system. Fig. 5 shows the forces acting on the parachute-payload system.

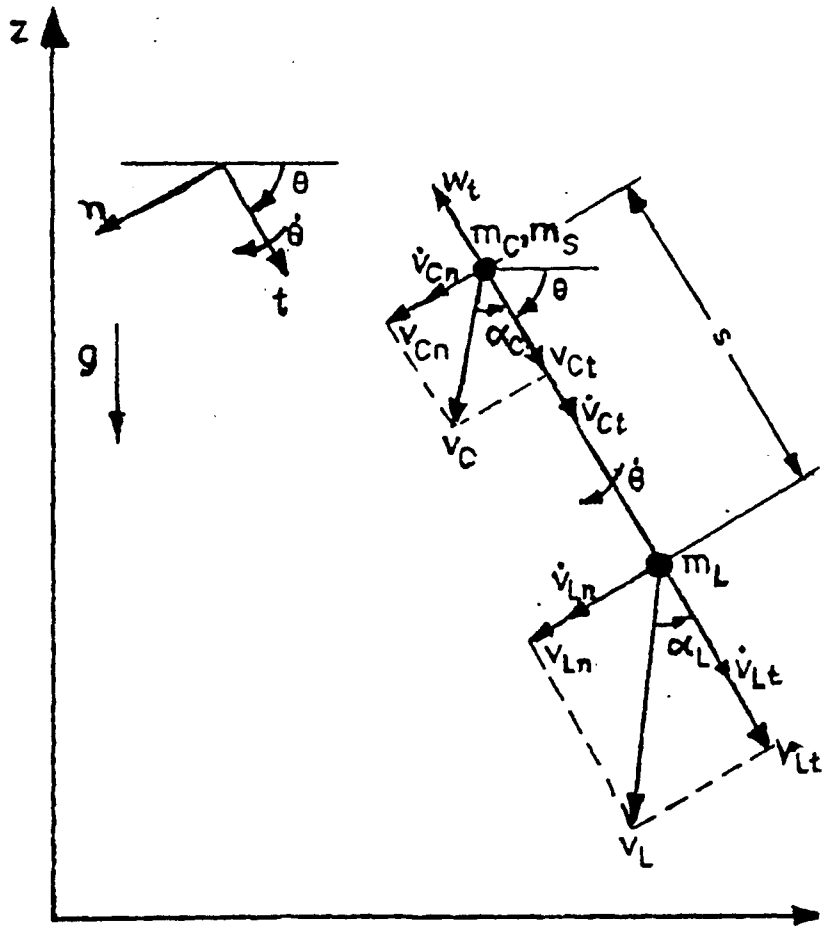

Fig. 4. Velocity and Acceleration Components of the Elastically Connected Canopy (m_C) and Payload (m_L) Mass Points in the Body Coordinate System [12].

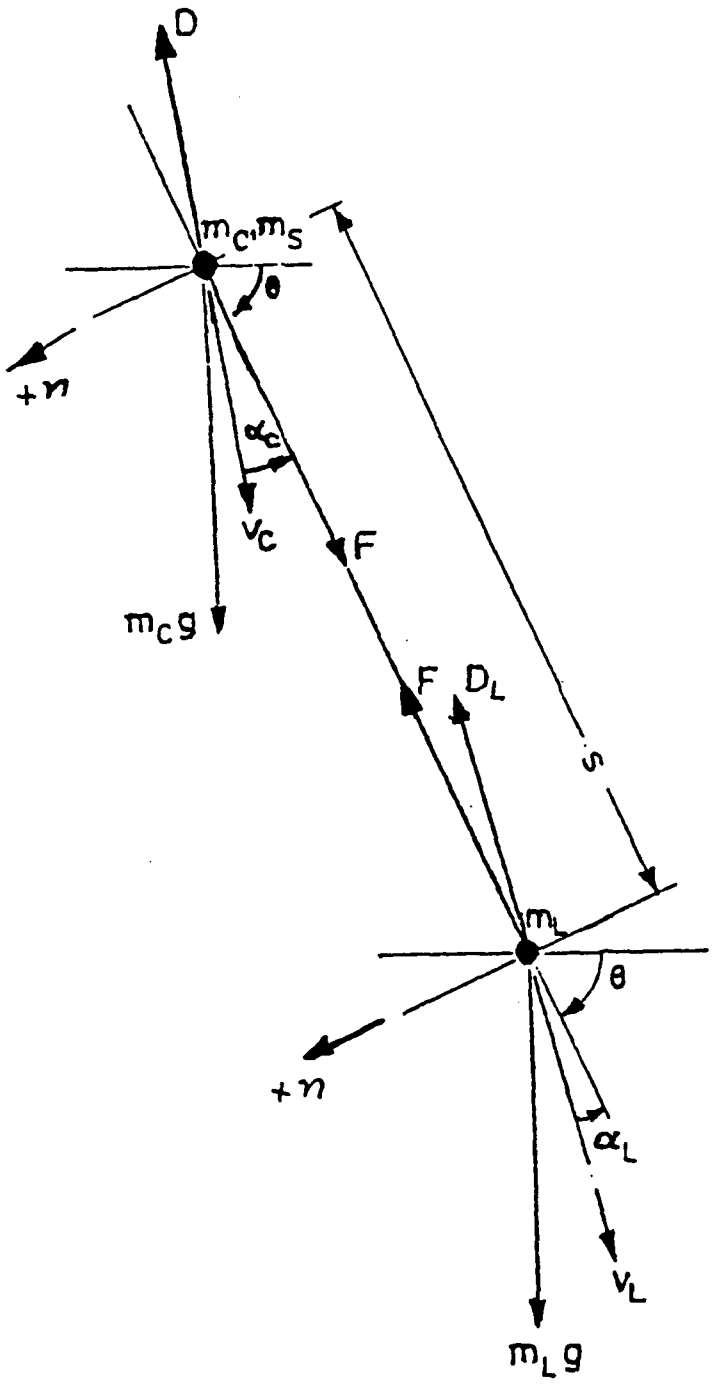

Fig. 5. Forces Acting on the Parachute-Payload System (Velocities also Shown) [12].

Computer program development

Each phase of the opening process involves the numerical solution of between five and eight simultaneous nonlinear differential equations, together with numerous geometric constraint equations.

To properly program the equations developed in [12], it is necessary to become thoroughly familiar with all the equation derivations; verifying assumptions, checking the algebra of the derivations, checking for typographical errors in the preparation of [12], and then coding the program into a computer language (in this case, Fortran was used). Because of the complexity of this task, and due to time limitations, it was not possible to do these steps for all three phases, and some compromises had to be made. These were as follows.

The first filling phase equations were checked carefully, some typographical errors were noted and corrected, and the equations were programmed. Because of time constraints, only some of the equations were checked for the second filling phase and transition phase. The major part of the effort went into programming these equations and running them to check if the results seemed reasonable.

One point should be made here. As the program goes from one filling phase to another, the relative velocity between the canopy and payload must be recalculated between phases and a small discontinuity in this value introduced. This discontinuity is necessary to satisfy force and length continuity in the suspension lines, between phases, due to the discontinuity that inevitably must occur when the geometric model is abruptly changed between phases. In most cases, the change in relative velocity is less than a few percent and should be of no consequence within the accuracy of the theory. This approximation is inherent to Fu's theory.

Current Limitations in the Program

There are two limitations in the computer program that should be removed at a later date. For certain calculated drop conditions, the calculated force in the suspension lines goes to a small negative value for a short period of time during the transition phase. During the transition phase, the parachute-payload is behaving primarily as a spring-mass-damper system. Conceivably this behavior could occur during the other phases for some drop conditions. Fu made no mention of how this should be handled in [12]. Obviously, this must be modified by program statements that set the suspension line force equal to zero if a negative force is calculated, since the suspension lines cannot physically tolerate a compressive force. In [5], Payne's theory also considers suspension line stiffness, but not canopy stiffness, and the suspension line force also goes to zero several times during some drops due to the spring-mass-damper characteristics of the system.

The other change that needs to be made to the program is an improvement in the accuracy of the integration routine used. The current program uses Euler's method for solving the differential equations. This is adequate as a first approximation to the theory, but needs to be upgraded before the program is used extensively. A higher order integration routine, such as fourth-order Runge-Kutta, should be incorporated. Additionally, time should be spent checking the accuracy of the remaining equations in [12] to ensure that no additional typographical or derivation errors exist.

Program Listing and Typical Output

Appendix A contains the Fortran listing for the program, temporarily called FUDROP here, with input for a typical case. The input is for a C-9 type parachute canopy, and the parachute geometry and drop conditions are given in Table 1. The values in Table 1 correspond to Example 1 from [12] and are used to compare this program's output with Fu's results.

Appendix B contains the program output for this case. The first part of the program is an echo of the input for parachute geometry and snatch conditions. This is followed by the output for the first filling phase, lasting for 0.20 seconds, followed by a statement indicating the end of the first filling phase.

Table 1. Parachute Geometry and Drop Conditions, FUDROP (See Appendix A)

Variable	Symbol	Value
Parachute nominal diameter	D_o	28.22 ft
Constructed diameter	D_C	28.45 ft
Payload radius	R	0.755 ft
Vent radius	R_V	0.820 ft
Suspension line length	l_s	28.22 ft
Air density (1000 ft alt)	ρ	0.00231 sl/ft^3
Number of suspension lines	n	28
Drag coefficient of payload	C_{DL}	0.64
Snatch velocity	V_s	185 fps
Total weight	W_T	296 lbs
Payload weight	W_L	280 lbs
Initial trajectory angle (below horizontal)	θ_o	50°
Snatch force	F_s	662 lbs
Effective porosity of fabric	C_{eff}	0.1

The output format for the second filling phase is presented in a slightly different arrangement, and ends at 0.90 seconds for this example. The output for the transition phase is again in a different format, and calculations for this case were stopped at 5.9 seconds, as the terminal velocity had essentially been reached and the trajectory was approximately vertical (Θ = 85°).

Comparison with Fu's Results

The calculated results from Appendix B are nondimensionalized and compared with Fu's results in Fig. 6. In this figure, the solid lines are Fu's calculated results, the short dashed lines drawn through squares, triangles or diamond-shaped symbols are the Appendix B results, and the long dashed lines are experimental data from [18]. The letters along the abscissa of Fig. 6 correspond to comparisons of the calculated and measured parachute shapes, semi-apertural angles, and nondimensional times in Fig. 7.

Figure 7 shows fair to good agreement between theory and experiment. The major difference is that the parachute changes shape somewhat at the beginning of the transition phase, including the well known "overexpansion." The theory does not account for this, nor for the change in suspension line angle during the first filling phase.

Comparing the results in Fig. 6 for nondimensional radius, $\overline{r}$, the Appendix B results differ from Fu's somewhat, but agree better with experiment. The present theory shows the parachute growing in size more slowly than Fu predicts. Comparing nondimensional velocity ($\overline{v}_L$) histories, Fu's theory agrees better with experiment than the Appendix B results. The slower theoretical parachute growth rate of the present theory results in less drag and a resulting slower velocity decay than predicted by Fu. For the force history comparison, Fu's results agree better with experiment during the early part of the opening time period, but the Appendix B results agree better with experiment near the peak period of the force history. Generally, the trends shown for both theories and the experiment agree well.

It is expected that better agreement between the present programming of Fu's theory (Appendix A) and Fu's results would be obtained if a more accurate integration routine were used in Appendix A. The type of deviation between the two theories shown in Fig. 6 is typical of the difference obtained when using Euler's method for integration as opposed to higher order methods.

Suggestions for future work

The present theory should be improved by updating the integration routine and incorporating program statements to set riser force equal to zero whenever the program calculates a negative suspension line force (this has occurred for the present theory only for short periods of time in the transition phase for cases examined thus far). The remaining equations developed by Fu should be checked for accuracy.

Fu applied this theory only to aircraft drop test data of full-scale 28 ft D_o C-9 parachutes. The program should be used to compare predictions with Lee's drop test data [19,20] for the 1/2-scale and 1/4-scale C-9 models, and to the full-scale C-9 parachutes that were drop tested with the heavier fabrics as part of Natick's scaling studies.

Finally, the program should be modified in some fashion to simulate canopy stiffness effects so the program can be better used to study the scaling problems that arise when using model wind tunnel or drop test data to predict prototype parachute performance. The program could then be used as a basis for further theoretical verification of the relative stiffness index proposed in [21].

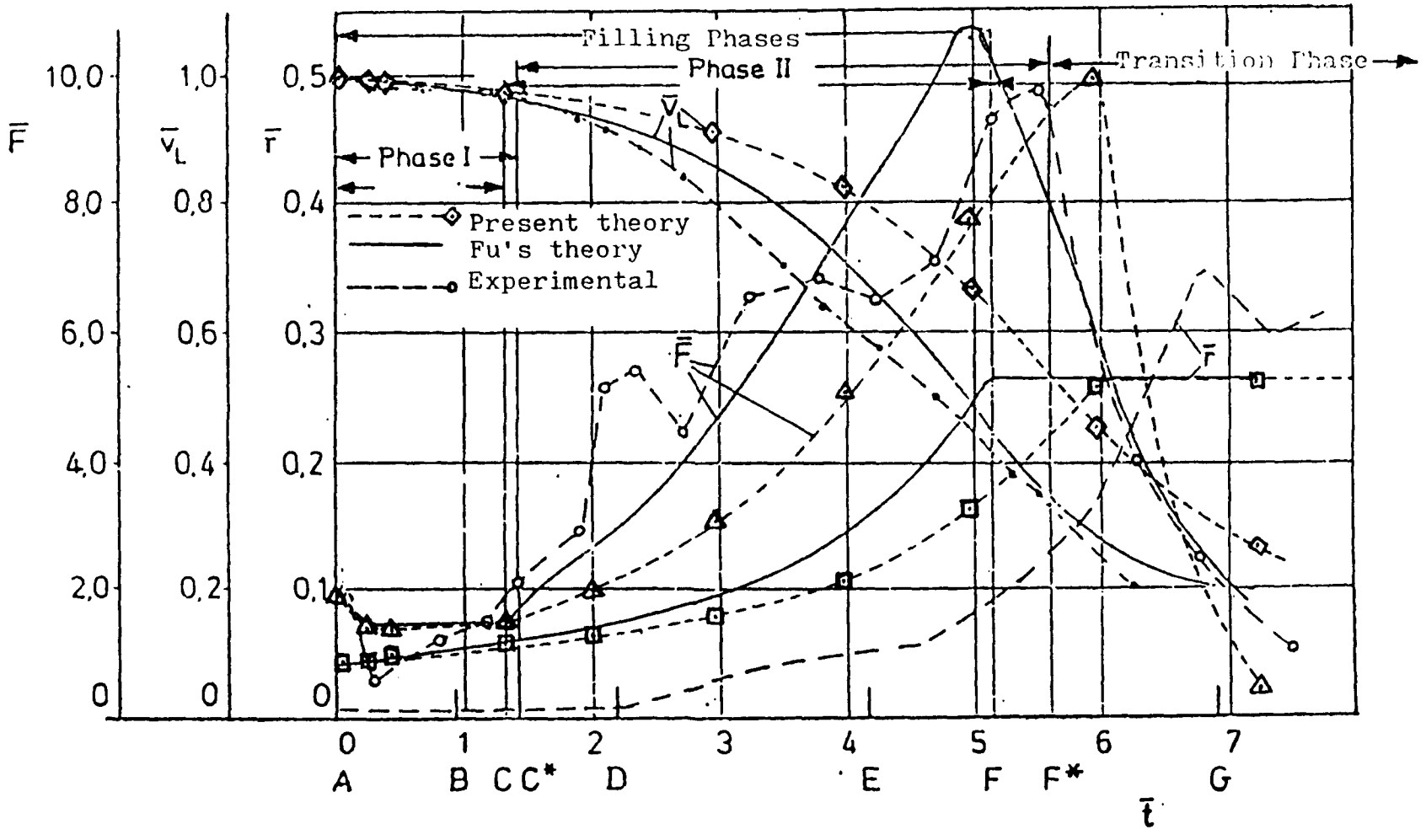

Fig. 6. Calculated and Measured Values of the Force F, Velocity $\bar{v}_L$, and Radius, $\bar{r}$ versus Time $\bar{t}$, in Nondimensional Form (Measurement results: [18], Figure: [12]).

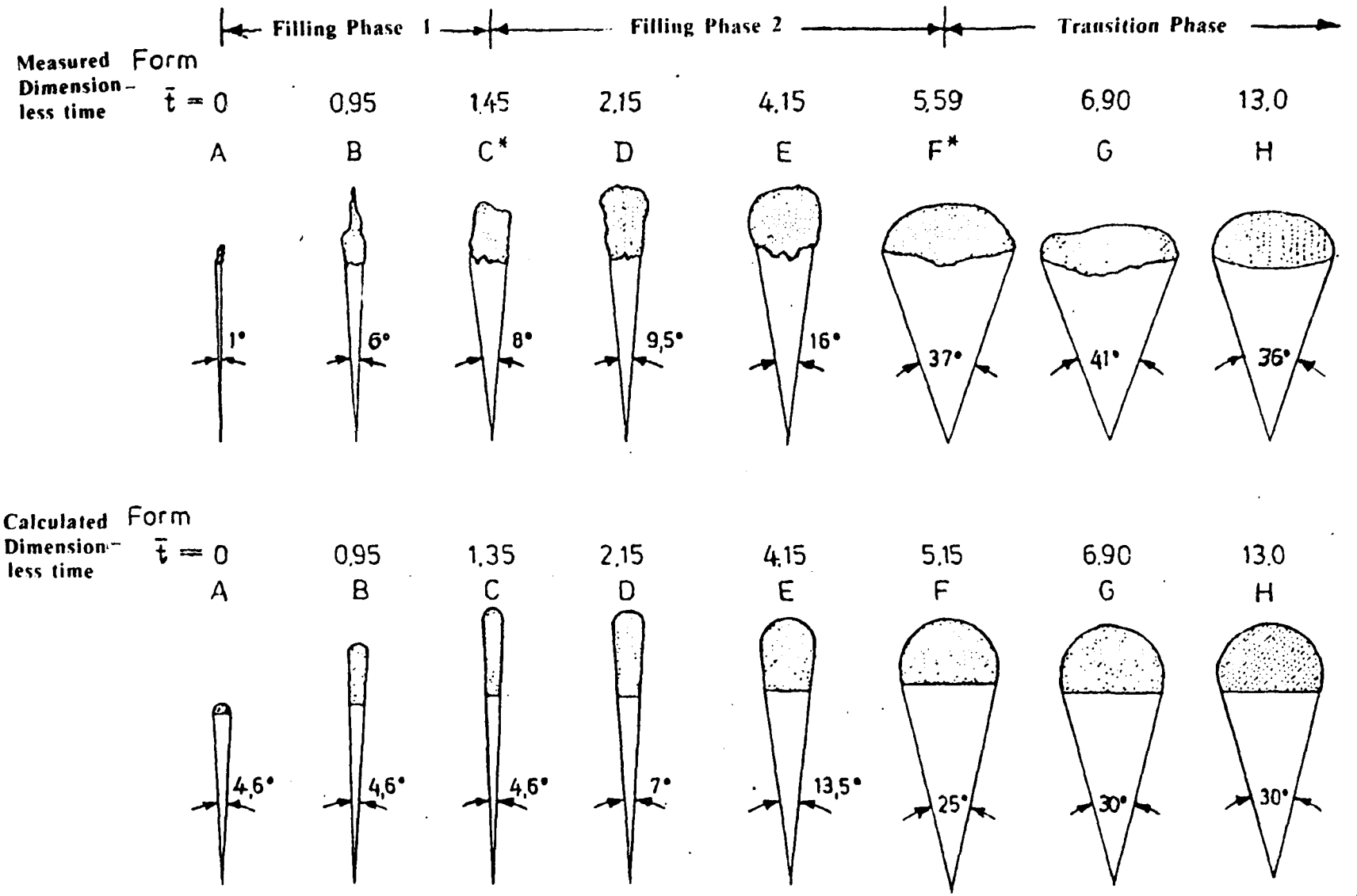

Fig 7. Calculated and Measured Geometric Shape of the Canopy at Various Nondimensional Times (Measurements: [18], Figure: [12]).

Conclusions

Any evaluation of experimental data on parachute scaling stiffness effects is somewhat hampered if a simplified theory is not available to guide in interpreting test data. This report has presented a theory that can be used for this purpose with suitable modifications.

The theory has been programmed in Fortran and checked against Fu's results for a single case. More work needs to be done to check the equation derivations and upgrade the integration routines.

After the improvements are made, the theory should be compared with available Natick drop test data on scale model parachutes, and the effects of canopy stiffness should be incorporated into the theory.

References

1. Niemi, E.E., "An Improved Scaling Law for Determining Stiffness of Flat Circular Parachute Canopies," Technical Report, IPA Research Project No. 05-5179, University of Lowell, Lowell, MA, January 1990.

2. Mueller, W., "Parachutes for Aircraft," *Zeitschrift fuer Flugteknik und Motorluft-schiffahrt*, Heft No. 20, 1927.

3. Weinig, F.S., "On the Dynamics of the Opening Shock of a Parachute," USAF Office of Aeronautical Research, WADC, Dayton, Ohio, TR-6, February 1951.

4. Roberts, B.W., "Aerodynamic Inflation of Shell Type Parachute Structures," *Journal of Aircraft*, Vol. 11, July 1974, pp. 390–397.

5. Payne, P.R., "A New Look at Parachute Opening Dynamics," *Aeronautical Journal*, Vol. 11, February 1973, pp. 85–93.

6. Wolf, D.F., "A Simplified Dynamic Model of Parachute Inflation," *Journal of Aircraft*, Vol. 11, January 1974, pp. 28–33.

7. McVey, D.F., and Wolf, D.F., "Analysis of Deployment and Inflation of Large Ribbon Parachutes," *Journal of Aircraft*, Vol. 11, February 1974, pp. 96–103.

8. O'Hara, F., "Notes on the Opening Behavior and the Opening Forces of Parachutes," *Royal Aeronautical Society Journal*, Nov. 1949, pp. 1053–1062.

9. Heinrich, H.G., and Bhateley, I.C., "A Simplified Analytical Method to Calculate Parachute Opening Time and Opening Shock," Summer Course on Aerodynamic Deceleration, University of Minnesota, July 1961.

10. Heinrich, H.G., "A Linearized Theory of Parachute Opening Dynamics," *Royal Aeronautical Society Journal*, Vol. 76, December 1972, pp. 723–730.

11. Heinrich, H.G., and Saari, D.P., "Parachute Opening Shock Calculations with Experimentally Established Input Functions," *Journal of Aircraft*, Vol. 15, No. 2, February 1978, pp. 100–105.

12. Fu, K-H., "Theoretical Study of the Filling Process of a Flexible Parachute Payload System," German Air and Space Research and Test Institute, Braunschweig, Germany, 1975.

13. Lingard, J.S., "The Aerodynamics of Parachutes During the Inflation Process," Ph.D. Thesis, Department of Aeronautical Engineering, University of Bristol, England, October 1978.

14. Roberts, B.W., and Reddy, K.R., "A Discussion of Parachute Inflation Theories," AIAA Paper No. 75-1351, November 17–19, 1975.

15. Ewing, E.G., Bixby, H.W., and Knacke, T.W., "Recovery Systems Design Guide," AFFDL-TR-78-151, December 1978.

16. Muramoto, K.K., and Garrard, W.L., "A Method for Calculating the Pressure Field about a Ribbon Parachute Canopy in Steady Descent," Proceedings of the 8th Aerodynamic Decelerator and Balloon Technology Conf., Hyannis, MA, April 1984, pp. 57–67.

17. Heinrich, H.G., and Hektner, T.R., "Flexibility as a Model Parachute Performance Parameter," *Journal of Aircraft*, Vol. 8, No. 5, Sept. 1971, p. 704.

18. Doukas, C., Lampe, M., and Schmidt, H.K., "Drop Experiments for the Project 'Scale Influences in Parachutes' with Canopies of the 'Circular Flat' Type," DFVLR, Aerodynamics Institute, Internal Report 154-74/2, 1974.

19. Lee, C.K., "Experimental Investigation of Full-Scale and Model Parachute Opening," Proceedings of the AIAA 8th Aerodynamic Decelerator and Balloon Technology Conference, New York, 1984, pp. 215–223.

20. Lee, C.K., "Modeling of Parachute Opening: An Experimental Investigation," *Journal of Aircraft*, Vol. 26, No. 5, May 1989, pp. 444–451.

21. Niemi, E.E., "An Improved Canopy Stiffness Scaling Law for Determining Opening Time of Flat Circular Parachutes," Proceedings of the AIAA 8th Applied Aerodynamics Conf., Portland, OR, August 20–22, 1990.

Appendix A

FORTRAN LISTING OF FUDROP PROGRAM

```
      PROGRAM FUDROP
C     THIS PROGRAM CALCULATES THE OPENING DYNAMICS OF A PARACHUTE
C     USING FU'S THEORY

C     THIS PORTION OF THE PROGRAM INCLUDES GEOMETRIC PARACHUTE INPUTS
C     AND INITIAL DEPLOYMENT CONDITIONS
      CF=20.6
      CEF=0.1
      CD1=0.5
      RP=0.755
      CD2=1.315
      CDL=0.64
      DS=1.37
      DO=28.22
      DC=28.45
      FS=662.
      G=32.19
      XK=2.
      XK1=0.49
      XLS=28.22
      XN=28.
      RV=0.82
      WL=280.
      WT=296.
      VS=185
      ZL=1000.
      BO=0.04
      P=3.1416
      THO=0.8727
      RM=0.
      RHO=0.00231
      XOMO=0.

      PRINT*,'THE DEFAULT INPUTS FOR THIS PROGRAM ARE AS FOLLOWS'
      PRINT*,'PARACHUTE DIAMETER IS',DO,'FT'
      PRINT*,'CONSTRUCTED DIA OF PARACHUTE IS',DC,'FT'
      PRINT*,'NO. OF SUSPENSION LINES IS',XN
      PRINT*,'SUSPENSION LINE LENGTH IS',XLS,'FT'
      PRINT*,'APERTURE RADIUS IS',RV,'FT'
      PRINT*,'EFFECTIVE POROSITY IS',CEF
      PRINT*,'SPRING CONSTANT OF A SUSPENSION LINE IS',CF,'LB/FT'
      PRINT*,'DAMPING COEF. OF A SUSP. LINE IS',DS,'LB-SEC/FT'
      PRINT*,'FIRST PHASE PARA. DRAG COEFF IS',CD1
      PRINT*,'SECOND PHASE PARA. DRAG COEFF IS',CD2
      PRINT*,'TOTAL CANOPY & PAYLOAD WEIGHT IS',WT,'LBS'
      PRINT*,'APP. MASS PROPORTIONALITY CONSTANT IS',XK
```

```
      PRINT*,'FIRST PHASE CONTRACTION FACTOR IS',XK1
      PRINT*,'INITIAL SEMI-APERTURE ANGLE IS',BO,'RADS'
      PRINT*,'PAYLOAD WEIGHT IS',WL,'LBS'
      PRINT*,'PAYLOAD RADIUS IS',RP,'FT'
      PRINT*,'PAYLOAD DRAG COEFF IS',CDL
      PRINT*,' '
      PRINT*,'PARACHUTE SNATCH CONDITIONS ARE AS FOLLOWS:'
      PRINT*,'SNATCH VELOCITY IS',VS,'FT/SEC'
      PRINT*,'INITIAL FLIGHT PATH ANGLE THETA IS',THO,'RADS'
      PRINT*,'X COORD OF PAYLOAD AT SNATCH IS',XL,'FT'
      PRINT*,'ALTITUDE OF PAYLOAD AT SNATCH IS',ZL,'FT'
      PRINT*,'OPENING SHOCK OF PAYLOAD AT SNATCH IS',FS,'LBS'
      PRINT*,'REL. VEL. BETWEEN CANOPY AND LOAD IS',RW,'FPS'
      PRINT*,'INITIAL ANG. ROTATION RATE IS',XOMO,'RAD/SEC'

C     INITIAL VALUES OF VARIABLES FOR FIRST FILLING PHASE
      DT=.001
      DTPR=.01
      TPR=DTPR
      VLT=VS
      VCN=0.
      TH=THO
      XOM=XOMO
      XLO=(FS/(XN*CF*COS(BO)))+XLS
      RO=((FS/(XN*CF*COS(BO)))+XLS)*TAN(BO)
      VO=((P/3.)*RO**3.)*(4.-(2.+SIN(BO))*(1.-SIN(BO))**2.)
      R=RO
      H=0.
      V=VO
      XL=XLO
      XML=WL/G
      XMC=(WT-WL)/G
      CD=CD1
      CBO=COS(BO)
      SBO=SIN(BO)
      TBO=TAN(BO)
      CTBO=1./TBO
500   DPR=(P*R**2.)*(4.-(2.+SBO)*(1.-SBO)**2.)+(P*H*CBO**3.)*
     C  (2.*R-H*TBO)
      DPH=(P*CBO**3.)*(R-H*TBO)**2.
      VD=(XK1*P*CBO**2.)*(VLT-RW)*(R-H*TBO)**2.
      RD=((RW/CBO)*DPH+VD)/(CTBO*DPH+DPR)
      HD=(VD*CTBO-RW*DPR/CBO)/(CTBO*DPH+DPR)
      XLD=RD*CTBO-HD
      THD=XOM
      DV=VLT-RW
```

```
      RCH=R*CTBO-H
      VLTD=VCN*XOM+(XOM**2.)*RCH*CBO-(XN*CBO/XML)*(CF*(RCH
     C  -XLS)+DS*RW/CBO)+G*SIN(TH)-(.5*CDL*RHO*VLT/XML)*SQRT(
     C  VLT**2.+(VCN+XOM*RCH*CBO)**2.)*P*RP**2.
      RWD=VLTD-VCN*XOM+((XK*RHO*DV*VD)/(XMC+XK*RHO*V))-((XN*
     C       CBO*(CF*(RCH-XLS)+DS*RW/CBO)+XMC*G*SIN(TH)-.5*CD*RHO
     C       *DV*SQRT(DV**2.+VCN**2.)*P*R**2.)/(XMC+XK*RHO*V))
        VCND=
     C   -DV*XOM-(XK*RHO*VCN*VD)/(XMC+XK*RHO*V)+(XMC*G*COS(
     C       TH)-.5*CD*RHO*VCN*SQRT(DV**2.+VCN**2.)*P*R**2.)/(XMC
     C       +XK*RHO*V)
      XOMD=(-VCND-(VLT+RW)*XOM+G*COS(TH)-(0.5*CDL*RHO/XML)
     C       *(VCN+XOM*RCH*CBO)*SQRT(VLT**2.+(VCN+XOM*RCH*CBO)**
     C       2.)*P*RP**2.)/(CBO*RCH)
      XL=R*CTBO-H
      XLD=RD*CTBO-HD
      F=XN*CBO*(CF*(XL-XLS)+DS*XLD)
600   IF(T-TPR) 610,630,630
610   CONTINUE
620   GO TO 660
630   PRINT*,' '
      PRINT*,'TIME RATE OF CHANGE OF VOLUME IS',VD,'CFS/S'
      PRINT*,'TIME RATE OF CHANGE OF RADIUS IS',RD,'FT/S'
      PRINT*,'TIME RATE OF CHANGE OF H IS',HD,'FT/S'
      PRINT*,'PAYLOAD TANGENTIAL ACC. IS',VLTD,'FPS/S'
      PRINT*,'ACCEL OF CANOPY WRT PLD IS',RWD,'FPS/S'
      PRINT*,'CANOPY NORMAL ACC. IS',VCND,'FPS/S'
      PRINT*,'RISER FORCE ACTING ON PAYLOAD IS',F,'LBS'
      PRINT*,' '
      PRINT*,'  TIME (SECS) ','  VOL(CUFT) ','        RADIUS(FT)',
     C     '     HEIGHT(FT)','       LENGTH(FT)'
      PRINT*,T,V,R,H,XL
      PRINT*,' THETA(DEG)','      VLT(FPS)','         RW(FPS)',
     C  '         VCN (FPS) ','  OMEGA(RAD/SEC)'
      TH=57.296*TH
      PRINT*,TH,VLT,RW,VCN,XOM
      PRINT*,' '
      TH=TH/57.296
650   TPR=TPR+DTPR
660   TEST=H+(P/2.+BO)*R
      IF (TEST.GE.(DC/2.)) GO TO 900
      V=V+VD*DT
      R=R+RD*DT
      H=H+HD*DT
      XL=XL+XLD*DT
      TH=TH+THD*DT
```

```
      VLT=VLT+VLTD*DT
      RW=RW+RWD*DT
      VCN=VCN+VCND*DT
      XOM=XOM+XOMD*DT
      THD=XOM
      T=T+DT
      IF(T.GE.0.3) GO TO 1000
      GO TO 500
900   PRINT*,'END OF FIRST FILLING PHASE'
1000  CONTINUE
C     THIS PORTION OF THE PROGRAM CALCULATES THE PARACHUTE
C     BEHAVIOR DURING THE SECOND FILLING PHASE
      PRINT*,' '
      PRINT*,'PARACHUTE DYNAMICS DURING SECOND FILLING PHASE'
      DT=.001
      DTPR=0.05
      TPR=T+DTPR
      CD=CD2
      B=BO

C     PROGRAM REENTERED HERE EACH TIME WITH NEW VALUE OF BETA
1500  CB=COS(B)
      SB=SIN(B)
      TB=TAN(B)
      CTB=1./TB
      GE=0.5*P+B
      GEO=0.5*DC-(.5*P+B)*R
      GEOM=R*CTB-GEO
      A1=CB*(CTB+GE)
      A2=(P*R**2.)*(4.-(2.+SB)*(1.-SB)**2.)+((P*CB**3.)/3.)*((-GE)*(0.75
     *  *R**2.+(1.5*R-TB*GEO)**2.)+GEO*(1.5*R+2.
     *  *(1.5*R-TB*GEO)*(1.5+TB*GE)))
      B1=-(R*CB*CTB**2.+SB*(R*CTB-GEO))
      B2=P*(R*CB)**3.+((2.*P*CB**3.)/3.)*GEO*(1.5*R-TB*GEO)*(R*TB-
     +  (GEO/CB**2.))-((P*CB**3.)/3.)*(R+3.*TB*GEO)*(0.75*R**2.+
     +  (1.5*R-TB*GEO)**2.)

      H=GEO
      IF(H.GT.0.1*DO) XK2=1.0
      IF(H.LE.0.1*DO) XK2=0.1+9.*H/DO
      IF(H.LE..03*DO) GO TO 2000
      IF(B.GT.BO) GO TO 1540

C     THIS PORTION OF PROGRAM ITERATES ON VALUE OF RW
C     NEEDED FOR TRANSITION FROM PHASE I TO PHASE II
1530  PRINT*,'ITERATION SEQUENCE FOR RW BETWEEN PHASES I AND II'
```

```
      PRINT*,'FINAL PHASE I RW EQUALS',RW,'FPS'
      CONTINUE

1540  VD=P*(VLT-RW)*XK2*(((R-GEO*TB)*CB)**2.-RV**2.-2.*CEF*R*R*(SB+
     +  SQRT(1.-(RV/R)**2.)))
      RD=(RW*B2-B1*VD)/(A1*B2-B1*A2)
      BD=(A1*VD-RW*A2)/(A1*B2-B1*A2)
      IF(ABS(B-BO).GE..00002) GO TO 1560
      TEMPLD=RD*(0.5*P+B+CTB)-R*BD*CTB**2.
      IF(ABS(XLD-TEMPLD).LE..001) GO TO 1550
      RW=RW-BD*XL*SB
      GO TO 1540
1550  CONTINUE
      PRINT*,'INITIAL PHASE II RW EQUALS',RW,'FPS'
      XLD=TEMPLD
C     END OF ITERATION ROUTINE FOR RW BETWEEN PHASES I AND II

1560  THD=XOM
      VLTD=VCN*XOM+(GEOM)*CB*XOM**2.-((XN*CB)/XML)*(CF*(GEOM-XLS)
     +  +(DS*RW/CB)+DS*(GEOM)*BD*TB)+G*SIN(TH)-((CDL*RHO*VLT)/(2.*XML))
     +       *(SQRT(VLT**2.+(VCN+XOM*GEOM*CB)**2.))*P*RP**2.
      DV=VLT-RW
      RWD=VLTD-VCN*XOM+(XK*RHO*DV*VD)/(XMC+XK*RHO*V)-((XN*CB)*(CF*
     +       (GEOM-XLS)+DS*RW/CB+DS*GEOM*BD*TB)+XMC*G*SIN(TH)-0.5*CD*RHO
     +       *DV*(SQRT(DV**2.+VCN**2.))*P*R**2.)/(XMC+XK*RHO*V)
      VCND=-DV*XOM-(XK*RHO*VCN*VD)/(XMC+XK*RHO*V)+(XMC*G*COS(TH)
     +  -0.5*CD*RHO*VCN*(SQRT(DV**2.+VCN**2.))*P*R**2.)/(XMC+XK*RHO*V)
      XOMD=(-VCND-(VLT+RW)*XOM+G*COS(TH)-(0.5*CDL*RHO/XML)*(VCN+XOM
     +       *GEOM*CB)*(SQRT(VLT**2.+(VCN+XOM*GEOM*CB)**2.))*P*RP**2.)/(
     +  CB*GEOM)
      F=XN*CB*(CF*(R*CTB-H-XLS)+DS*(RD*(0.5*P+B+CTB)-R*BD*CTB**2.))
1600  IF(T-TPR) 1610,1630,1630
1610  CONTINUE
1620  GO TO 1660
1630  PRINT*,' '
      PRINT*,'  TIME(SECS) ','  BETA(DEG) ', '       VOL(CUFT)','
     +  RADIUS(FT)',                '       FORCE(LBS)'

      B=57.296*B
      PRINT*,T,B,V,R,F
      B=B/57.296

      PRINT*,' THETA(DEG)','      VLT(FPS)','       RW(FPS)',
     +  '          VCN(FPS) ','   OMEGA(RAD/SEC)'
      TH=57.296*TH
      PRINT*,TH,VLT,RW,VCN,XOM
```

```
      PRINT*,' '
1650  TPR=TPR+DTPR
      TH=TH/57.296
1660  V=V+VD*DT
      R=R+RD*DT
      B=B+BD*DT
      TH=TH+THD*DT
      VLT=VLT+VLTD*DT
      RW=RW+RWD*DT
      VCN=VCN+VCND*DT
      XOM=XOM+XOMD*DT
      T=T+DT
      IF(T.GE.5.) GO TO 2500
      GO TO 1500
2000  PRINT*,'END OF SECOND FILLING PHASE'
C     THIS PORTION OF THE PROGRAM CALCULATES PARACHUTE BEHAVIOR
C     DURING THE TRANSITION PHASE
      PRINT*,' '
      PRINT*,'BEGINNING OF TRANSITION PHASE'
      PRINT*,' '
      DT=.001
      DTPR=0.1
      TPR=T+DTPR
      RST=R
      HST=H
      BST=B
      VST=V
      PRINT*,'STEADY STATE CANOPY VOLUME EQUALS',VST,'CU FT'
      PRINT*,'STEADY STATE CANOPY RADIUS EQUALS',RST,'FT'
      PRINT*,'HST EQUALS',HST,'FT. AND BETAST EQUALS',BST,'RADS'
      PRINT*,' '
      CONS=RST*COS(BST)-HST*SIN(BST)
      SB=SIN(B)
      CB=COS(B)
      TB=TAN(B)
      CTB=1./TB
      XL=CONS/SB
C     THIS PORTION OF PROGRAM CALCULATES A NEW VALUE OF RW
C     NEEDED FOR FORCE CONTINUITY BETWEEN PHASE II AND
C     TRANSITION PHASE
      PRINT*,'FINAL PHASE II RW EQUALS',RW,'FPS'
      RW=F/(XN*DS*CB**2.)-CF*(XL-XLS)/(DS*CB)
      PRINT*,'INITIAL VALUE FOR RW FOR TRANS. PHASE EQ',RW,'FPS'
1700  SB=SIN(B)
      CB=COS(B)
      TB=TAN(B)
```

```
      CTB=1./TB
      XL=CONS/SB
      XLD=RW*CB
      BD=-RW*SB/XL
      THD=XOM
      VLTD=VCN*XOM+XL*CB*XOM**2.-XN*CF*CB*(XL-XLS)/XML-(XN*DS*
     *  RW*CB**2.)/XML+G*SIN(TH)-(CDL*RHO*VLT*SQRT(VLT**2.+(VCN+
     +  XOM*XL*CB)**2.)*P*R**2.)/(2.*XML)
      RWD=VLTD-VCN*XOM-(XN*CB*CF*(XL-XLS)+XN*DS*RW*CB**2.+XMC*
     *  G*SIN(TH)-0.5*CD*RHO*(VLT-RW)*SQRT((VLT-RW)**2.+VCN**2.)
     *  *P*RST**2.)/(XMC+XK*RHO*VST)
      VCND=-(VLT-RW)*XOM+(XMC*G*COS(TH)-0.5*CD*RHO*VCN*SQRT(
     +  (VLT-RW)**2.+VCN**2.)*P*RST**2.)/(XMC+XK*RHO*VST)
      XOMD=(-VCND-(VLT+RW)*XOM+G*COS(TH)-(0.5*CDL*RHO*(VCN+XOM*
     *  XL*CB)*SQRT(VLT**2.+(VCN+XOM*XL*CB)**2.)*P*RP**2.)/XML)
     *  /(XL*CB)
      F=XN*CB*(CF*(XL-XLS)+DS*XLD)
1800  IF(T-TPR) 1810,1830,1830
1810  CONTINUE
1820  GO TO 1860
1830  PRINT*,' '
      PRINT*,'TIME(SECS)','        BETA(DEG)'   ,'       FORCE(LBS)',
     +  '    VLT(FPS)','   LENGTH(FT)'
      B=57.296*B
      PRINT*,T,B,F,VLT,XL
      B=B/57.296
      PRINT*,'THETA(DEG)','        RW(FPS)' ,        '        VCN(FPS)',
     +  '        OMEGA(RD/SEC)'
      TH=57.296*TH
      PRINT*,TH,RW,VCN,XOM
      PRINT*,' '
1850  TPR=TPR+DTPR
      TH=TH/57.296
1860  B=B+BD*DT
      VLT=VLT+VLTD*DT
      TH=TH+THD*DT
      RW=RW+RWD*DT
      VCN=VCN+VCND*DT
      XOM=XOM+XOMD*DT
      T=T+DT
      IF(T.GE.6.0) GO TO 2500
      GO TO 1700
2500  CONTINUE
      STOP
      END
```

Appendix B

EXAMPLE FUDROP PROGRAM OUTPUT

```
THE DEFAULT INPUTS FOR THIS PROGRAM ARE AS FOLLOWS
PARACHUTE DIAMETER IS     28.2200FT
CONSTRUCTED DIA OF PARACHUTE IS     28.4500FT
NO. OF SUSPENSION LINES IS     28.0000
SUSPENSION LINE LENGTH IS     28.2200FT
APERTURE RADIUS IS    0.820000FT
EFFECTIVE POROSITY IS     1.00000E-01
SPRING CONSTANT OF A SUSPENSION LINE IS     20.6000LB/FT
DAMPING COEF. OF A SUSP. LINE IS     1.37000LB-SEC/FT
FIRST PHASE PARA. DRAG COEFF IS    0.500000
SECOND PHASE PARA. DRAG COEFF IS     1.31500
TOTAL CANOPY & PAYLOAD WEIGHT IS     296.000LBS
APP. MASS PROPORTIONALITY CONSTANT IS     2.00000
FIRST PHASE CONTRACTION FACTOR IS    0.490000
INITIAL SEMI-APERTURE ANGLE IS     4.00000E-02RADS
PAYLOAD WEIGHT IS     280.000LBS
PAYLOAD RADIUS IS    0.755000FT
PAYLOAD DRAG COEFF IS    0.640000

PARACHUTE SNATCH CONDITIONS ARE AS FOLLOWS:
SNATCH VELOCITY IS     185.000FT/SEC
INITIAL FLIGHT PATH ANGLE THETA IS    0.872700RADS
X COORD OF PAYLOAD AT SNATCH IS   0.FT
ALTITUDE OF PAYLOAD AT SNATCH IS    1000.000FT
OPENING SHOCK OF PAYLOAD AT SNATCH IS     662.000LBS
REL. VEL. BETWEEN CANOPY AND LOAD IS   0.FPS
INITIAL ANG. ROTATION RATE IS   0.RAD/SEC

TIME RATE OF CHANGE OF VOLUME IS     399.008CFS/S
TIME RATE OF CHANGE OF RADIUS IS     3.09262FT/S
TIME RATE OF CHANGE OF H IS     80.9260FT/S
PAYLOAD TANGENTIAL ACC. IS    -39.2486FPS/S
ACCEL OF CANOPY WRT PLD IS    -194.357FPS/S
CANOPY NORMAL ACC. IS     18.3940FPS/S
RISER FORCE ACTING ON PAYLOAD IS     510.826LBS

  TIME (SECS)    VOL(CUFT)         RADIUS(FT)     HEIGHT(FT)       LENGTH(FT)
    1.00000E-02     7.56761     1.20761    0.825014     29.3492
 THETA(DEG)      VLT(FPS)          RW(FPS)          VCN (FPS)    OMEGA(RAD/SEC)
    50.0023     184.523    -3.64878    0.192856     4.67598E-04


TIME RATE OF CHANGE OF VOLUME IS     399.535CFS/S
TIME RATE OF CHANGE OF RADIUS IS     2.91037FT/S
TIME RATE OF CHANGE OF H IS     77.5262FT/S
PAYLOAD TANGENTIAL ACC. IS    -31.2931FPS/S
```

```
ACCEL OF CANOPY WRT PLD IS   -42.1879FPS/S
CANOPY NORMAL ACC. IS    16.8182FPS/S
RISER FORCE ACTING ON PAYLOAD IS    441.804LBS

  TIME (SECS)    VOL(CUFT)         RADIUS(FT)     HEIGHT(FT)       LENGTH(FT)
    2.00000E-02     11.5629     1.23768     1.61925     29.3062
 THETA(DEG)      VLT(FPS)          RW(FPS)          VCN (FPS)    OMEGA(RAD/SEC)
    50.0028     184.171    -4.80202    0.369653     1.43896E-03


TIME RATE OF CHANGE OF VOLUME IS    397.765CFS/S
TIME RATE OF CHANGE OF RADIUS IS    2.76587FT/S
TIME RATE OF CHANGE OF H IS    74.0037FT/S
PAYLOAD TANGENTIAL ACC. IS   -27.6413FPS/S
ACCEL OF CANOPY WRT PLD IS    21.7000FPS/S
CANOPY NORMAL ACC. IS    15.3081FPS/S
RISER FORCE ACTING ON PAYLOAD IS    410.197LBS

  TIME (SECS)    VOL(CUFT)         RADIUS(FT)     HEIGHT(FT)       LENGTH(FT)
    3.00000E-02     15.5514     1.26611     2.37862     29.2572
 THETA(DEG)      VLT(FPS)          RW(FPS)          VCN (FPS)    OMEGA(RAD/SEC)
    50.0040     183.877    -4.88980    0.530984     2.86631E-03


TIME RATE OF CHANGE OF VOLUME IS    394.902CFS/S
TIME RATE OF CHANGE OF RADIUS IS    2.63271FT/S
TIME RATE OF CHANGE OF H IS    70.2807FT/S
PAYLOAD TANGENTIAL ACC. IS   -25.9111FPS/S
ACCEL OF CANOPY WRT PLD IS    47.6458FPS/S
CANOPY NORMAL ACC. IS    13.7209FPS/S
RISER FORCE ACTING ON PAYLOAD IS    395.317LBS

  TIME (SECS)    VOL(CUFT)         RADIUS(FT)     HEIGHT(FT)       LENGTH(FT)
    4.10000E-02     19.9129     1.29585     3.17383     29.2051
 THETA(DEG)      VLT(FPS)          RW(FPS)          VCN (FPS)    OMEGA(RAD/SEC)
    50.0064     183.583    -4.49456    0.691370     4.90619E-03


TIME RATE OF CHANGE OF VOLUME IS    392.139CFS/S
TIME RATE OF CHANGE OF RADIUS IS    2.52727FT/S
TIME RATE OF CHANGE OF H IS    67.1337FT/S
PAYLOAD TANGENTIAL ACC. IS   -25.3192FPS/S
ACCEL OF CANOPY WRT PLD IS    53.6420FPS/S
CANOPY NORMAL ACC. IS    12.3388FPS/S
RISER FORCE ACTING ON PAYLOAD IS    390.331LBS
```

```
  TIME (SECS)    VOL(CUFT)         RADIUS(FT)     HEIGHT(FT)       LENGTH(FT)
    5.10000E-02     23.8495     1.32169     3.86228     29.1623
 THETA(DEG)      VLT(FPS)          RW(FPS)          VCN (FPS)    OMEGA(RAD/SEC)
    50.0097     183.327    -3.98250    0.822314     7.13979E-03


TIME RATE OF CHANGE OF VOLUME IS     389.489CFS/S
TIME RATE OF CHANGE OF RADIUS IS     2.43277FT/S
TIME RATE OF CHANGE OF H IS     64.2371FT/S
PAYLOAD TANGENTIAL ACC. IS    -25.1769FPS/S
ACCEL OF CANOPY WRT PLD IS     52.4640FPS/S
CANOPY NORMAL ACC. IS     11.0085FPS/S
RISER FORCE ACTING ON PAYLOAD IS     389.269LBS

  TIME (SECS)    VOL(CUFT)         RADIUS(FT)     HEIGHT(FT)       LENGTH(FT)
    6.10000E-02     27.7588     1.34653     4.52037     29.1249
 THETA(DEG)      VLT(FPS)          RW(FPS)          VCN (FPS)    OMEGA(RAD/SEC)
    50.0145     183.075    -3.44765    0.939675     9.69320E-03


TIME RATE OF CHANGE OF VOLUME IS     387.047CFS/S
TIME RATE OF CHANGE OF RADIUS IS     2.34695FT/S
TIME RATE OF CHANGE OF H IS     61.5851FT/S
PAYLOAD TANGENTIAL ACC. IS    -25.2596FPS/S
ACCEL OF CANOPY WRT PLD IS     48.2936FPS/S
CANOPY NORMAL ACC. IS     9.72485FPS/S
RISER FORCE ACTING ON PAYLOAD IS     390.181LBS

  TIME (SECS)    VOL(CUFT)         RADIUS(FT)     HEIGHT(FT)       LENGTH(FT)
    7.10000E-02     31.6425     1.37046     5.15061     29.0927
 THETA(DEG)      VLT(FPS)          RW(FPS)          VCN (FPS)    OMEGA(RAD/SEC)
    50.0207     182.823    -2.94032     1.04395     1.25305E-02


TIME RATE OF CHANGE OF VOLUME IS     384.837CFS/S
TIME RATE OF CHANGE OF RADIUS IS     2.26833FT/S
TIME RATE OF CHANGE OF H IS     59.1605FT/S
PAYLOAD TANGENTIAL ACC. IS    -25.4541FPS/S
ACCEL OF CANOPY WRT PLD IS     43.0858FPS/S
CANOPY NORMAL ACC. IS     8.48377FPS/S
RISER FORCE ACTING ON PAYLOAD IS     392.082LBS

  TIME (SECS)    VOL(CUFT)         RADIUS(FT)     HEIGHT(FT)       LENGTH(FT)
    8.10000E-02     35.5028     1.39357     5.75537     29.0654
 THETA(DEG)      VLT(FPS)          RW(FPS)          VCN (FPS)    OMEGA(RAD/SEC)
    50.0287     182.570    -2.48043     1.13558     1.56191E-02
```

```
TIME RATE OF CHANGE OF VOLUME IS    383.043CFS/S
TIME RATE OF CHANGE OF RADIUS IS    2.20285FT/S
TIME RATE OF CHANGE OF H IS    57.1556FT/S
PAYLOAD TANGENTIAL ACC. IS   -25.6750FPS/S
ACCEL OF CANOPY WRT PLD IS    38.2766FPS/S
CANOPY NORMAL ACC. IS    7.40056FPS/S
RISER FORCE ACTING ON PAYLOAD IS    394.208LBS

  TIME (SECS)    VOL(CUFT)         RADIUS(FT)     HEIGHT(FT)       LENGTH(FT)
    9.00000E-02     38.9591     1.41372     6.27968     29.0446
 THETA(DEG)      VLT(FPS)         RW(FPS)         VCN (FPS)    OMEGA(RAD/SEC)
    50.0374     182.340    -2.11197     1.20758     1.85896E-02


TIME RATE OF CHANGE OF VOLUME IS    381.249CFS/S
TIME RATE OF CHANGE OF RADIUS IS    2.13520FT/S
TIME RATE OF CHANGE OF H IS    55.1055FT/S
PAYLOAD TANGENTIAL ACC. IS   -25.9419FPS/S
ACCEL OF CANOPY WRT PLD IS    33.1880FPS/S
CANOPY NORMAL ACC. IS    6.23221FPS/S
RISER FORCE ACTING ON PAYLOAD IS    396.776LBS

  TIME (SECS)    VOL(CUFT)         RADIUS(FT)     HEIGHT(FT)       LENGTH(FT)
    1.00000E-01     42.7813     1.43544     6.84186     29.0251
 THETA(DEG)      VLT(FPS)         RW(FPS)         VCN (FPS)    OMEGA(RAD/SEC)
    50.0490     182.082    -1.75242     1.27629     2.20776E-02


TIME RATE OF CHANGE OF VOLUME IS    379.642CFS/S
TIME RATE OF CHANGE OF RADIUS IS    2.07231FT/S
TIME RATE OF CHANGE OF H IS    53.2231FT/S
PAYLOAD TANGENTIAL ACC. IS   -26.2143FPS/S
ACCEL OF CANOPY WRT PLD IS    28.5380FPS/S
CANOPY NORMAL ACC. IS    5.09906FPS/S
RISER FORCE ACTING ON PAYLOAD IS    399.410LBS

  TIME (SECS)    VOL(CUFT)         RADIUS(FT)     HEIGHT(FT)       LENGTH(FT)
     0.110000     46.5864     1.45651     7.38432     29.0090
 THETA(DEG)      VLT(FPS)         RW(FPS)         VCN (FPS)    OMEGA(RAD/SEC)
    50.0625     181.821    -1.44187     1.33349     2.57392E-02


TIME RATE OF CHANGE OF VOLUME IS    378.201CFS/S
TIME RATE OF CHANGE OF RADIUS IS    2.01362FT/S
```

```
TIME RATE OF CHANGE OF H IS     51.4902FT/S
PAYLOAD TANGENTIAL ACC. IS    -26.4815FPS/S
ACCEL OF CANOPY WRT PLD IS     24.3893FPS/S
CANOPY NORMAL ACC. IS     3.99957FPS/S
RISER FORCE ACTING ON PAYLOAD IS     402.019LBS

  TIME (SECS)    VOL(CUFT)         RADIUS(FT)     HEIGHT(FT)       LENGTH(FT)
   0.120000     50.3762     1.47696     7.90863     28.9958
 THETA(DEG)      VLT(FPS)          RW(FPS)          VCN (FPS)    OMEGA(RAD/SEC)
    50.0783     181.558    -1.17557     1.37950     2.95522E-02


TIME RATE OF CHANGE OF VOLUME IS     376.902CFS/S
TIME RATE OF CHANGE OF RADIUS IS     1.95871FT/S
TIME RATE OF CHANGE OF H IS     49.8908FT/S
PAYLOAD TANGENTIAL ACC. IS    -26.7384FPS/S
ACCEL OF CANOPY WRT PLD IS     20.7359FPS/S
CANOPY NORMAL ACC. IS     2.93252FPS/S
RISER FORCE ACTING ON PAYLOAD IS     404.557LBS

  TIME (SECS)    VOL(CUFT)         RADIUS(FT)     HEIGHT(FT)       LENGTH(FT)
   0.130000     54.1522     1.49685     8.41623     28.9851
 THETA(DEG)      VLT(FPS)          RW(FPS)          VCN (FPS)    OMEGA(RAD/SEC)
    50.0962     181.292   -0.948496     1.41467     3.34964E-02


TIME RATE OF CHANGE OF VOLUME IS     375.725CFS/S
TIME RATE OF CHANGE OF RADIUS IS     1.90717FT/S
TIME RATE OF CHANGE OF H IS     48.4103FT/S
PAYLOAD TANGENTIAL ACC. IS    -26.9811FPS/S
ACCEL OF CANOPY WRT PLD IS     17.5555FPS/S
CANOPY NORMAL ACC. IS     1.89695FPS/S
RISER FORCE ACTING ON PAYLOAD IS     406.991LBS

  TIME (SECS)    VOL(CUFT)         RADIUS(FT)     HEIGHT(FT)       LENGTH(FT)
   0.140000     57.9159     1.51620     8.90839     28.9765
 THETA(DEG)      VLT(FPS)          RW(FPS)          VCN (FPS)    OMEGA(RAD/SEC)
    50.1164     181.023   -0.755820     1.43931     3.75531E-02


TIME RATE OF CHANGE OF VOLUME IS     374.653CFS/S
TIME RATE OF CHANGE OF RADIUS IS     1.85870FT/S
TIME RATE OF CHANGE OF H IS     47.0362FT/S
PAYLOAD TANGENTIAL ACC. IS    -27.2088FPS/S
ACCEL OF CANOPY WRT PLD IS     14.7971FPS/S
CANOPY NORMAL ACC. IS    0.892078FPS/S
```

```
RISER FORCE ACTING ON PAYLOAD IS    409.312LBS

  TIME (SECS)    VOL(CUFT)         RADIUS(FT)     HEIGHT(FT)       LENGTH(FT)
   0.150000     61.6682     1.53505     9.38622     28.9697
 THETA(DEG)      VLT(FPS)          RW(FPS)          VCN (FPS)    OMEGA(RAD/SEC)
    50.1390     180.752   -0.593041     1.45373     4.17051E-02


TIME RATE OF CHANGE OF VOLUME IS    373.669CFS/S
TIME RATE OF CHANGE OF RADIUS IS    1.81300FT/S
TIME RATE OF CHANGE OF H IS    45.7572FT/S
PAYLOAD TANGENTIAL ACC. IS   -27.4205FPS/S
ACCEL OF CANOPY WRT PLD IS    12.4195FPS/S
CANOPY NORMAL ACC. IS   -8.27179E-02FPS/S
RISER FORCE ACTING ON PAYLOAD IS    411.510LBS

  TIME (SECS)    VOL(CUFT)         RADIUS(FT)     HEIGHT(FT)       LENGTH(FT)
   0.160000     65.4102     1.55343     9.85075     28.9644
 THETA(DEG)      VLT(FPS)          RW(FPS)          VCN (FPS)    OMEGA(RAD/SEC)
    50.1640     180.479   -0.456084     1.45824     4.59368E-02


TIME RATE OF CHANGE OF VOLUME IS    372.760CFS/S
TIME RATE OF CHANGE OF RADIUS IS    1.76983FT/S
TIME RATE OF CHANGE OF H IS    44.5637FT/S
PAYLOAD TANGENTIAL ACC. IS   -27.6166FPS/S
ACCEL OF CANOPY WRT PLD IS   10.37396FPS/S
CANOPY NORMAL ACC. IS   -1.02798FPS/S
RISER FORCE ACTING ON PAYLOAD IS    413.589LBS

  TIME (SECS)    VOL(CUFT)         RADIUS(FT)     HEIGHT(FT)       LENGTH(FT)
   0.170000     69.1428     1.57137    10.30289     28.9603
 THETA(DEG)      VLT(FPS)          RW(FPS)          VCN (FPS)    OMEGA(RAD/SEC)
    50.1914     180.204   -0.341355     1.45314     5.02336E-02


TIME RATE OF CHANGE OF VOLUME IS    371.914CFS/S
TIME RATE OF CHANGE OF RADIUS IS    1.72896FT/S
TIME RATE OF CHANGE OF H IS    43.4470FT/S
PAYLOAD TANGENTIAL ACC. IS   -27.7969FPS/S
ACCEL OF CANOPY WRT PLD IS    8.62326FPS/S
CANOPY NORMAL ACC. IS   -1.94417FPS/S
RISER FORCE ACTING ON PAYLOAD IS    415.545LBS

  TIME (SECS)    VOL(CUFT)         RADIUS(FT)     HEIGHT(FT)       LENGTH(FT)
   0.180000     72.8665     1.58888     10.7434     28.9574
```

```
 THETA(DEG)      VLT(FPS)         RW(FPS)         VCN (FPS)    OMEGA(RAD/SEC)
    50.2213     179.927  -0.245714     1.43871     5.45820E-02


TIME RATE OF CHANGE OF VOLUME IS     371.122CFS/S
TIME RATE OF CHANGE OF RADIUS IS     1.69022FT/S
TIME RATE OF CHANGE OF H IS     42.3995FT/S
PAYLOAD TANGENTIAL ACC. IS    -27.9618FPS/S
ACCEL OF CANOPY WRT PLD IS     7.13040FPS/S
CANOPY NORMAL ACC. IS    -2.83169FPS/S
RISER FORCE ACTING ON PAYLOAD IS     417.381LBS

  TIME (SECS)    VOL(CUFT)         RADIUS(FT)     HEIGHT(FT)       LENGTH(FT)
    0.190000     76.5821     1.60599     11.1731     28.9553
 THETA(DEG)      VLT(FPS)         RW(FPS)         VCN (FPS)    OMEGA(RAD/SEC)
    50.2537     179.648  -0.166398     1.41525     5.89698E-02


TIME RATE OF CHANGE OF VOLUME IS     370.373CFS/S
TIME RATE OF CHANGE OF RADIUS IS     1.65342FT/S
TIME RATE OF CHANGE OF H IS     41.4146FT/S
PAYLOAD TANGENTIAL ACC. IS    -28.1125FPS/S
ACCEL OF CANOPY WRT PLD IS     5.85687FPS/S
CANOPY NORMAL ACC. IS    -3.69090FPS/S
RISER FORCE ACTING ON PAYLOAD IS     419.106LBS

  TIME (SECS)    VOL(CUFT)         RADIUS(FT)     HEIGHT(FT)       LENGTH(FT)
    0.200000     80.2899     1.62273     11.5927     28.9539
 THETA(DEG)      VLT(FPS)         RW(FPS)         VCN (FPS)    OMEGA(RAD/SEC)
    50.2887     179.368   -1.01000E-01     1.38305     6.33854E-02

END OF FIRST FILLING PHASE

PARACHUTE DYNAMICS DURING SECOND FILLING PHASE
ITERATION SEQUENCE FOR RW BETWEEN PHASES I AND II
FINAL PHASE I RW EQUALS    -9.51428E-02FPS
INITIAL PHASE II RW EQUALS   -0.129291FPS

  TIME(SECS)    BETA(DEG)        VOL(CUFT)          RADIUS(FT)        FORCE(LBS)
    0.251000     2.38648     86.9940     1.68810     486.851
 THETA(DEG)      VLT(FPS)         RW(FPS)         VCN(FPS)     OMEGA(RAD/SEC)
    50.5067     177.710    0.890433     1.08485     8.61435E-02


  TIME(SECS)    BETA(DEG)        VOL(CUFT)          RADIUS(FT)        FORCE(LBS)
    0.302000     2.50958     95.7100     1.77206     550.802
```

THETA(DEG)	VLT(FPS)	RW(FPS)	VCN(FPS)	OMEGA(RAD/SEC)
50.7894	175.723	1.55725	0.624452	0.107459

TIME(SECS)	BETA(DEG)	VOL(CUFT)	RADIUS(FT)	FORCE(LBS)
0.351999	2.66439	107.260	1.87782	629.700

THETA(DEG)	VLT(FPS)	RW(FPS)	VCN(FPS)	OMEGA(RAD/SEC)
51.1238	173.383	2.15085	6.96175E-02	0.125828

TIME(SECS)	BETA(DEG)	VOL(CUFT)	RADIUS(FT)	FORCE(LBS)
0.401998	2.86154	122.839	2.01220	729.786

THETA(DEG)	VLT(FPS)	RW(FPS)	VCN(FPS)	OMEGA(RAD/SEC)
51.5060	170.548	2.80460	-0.524261	0.140606

TIME(SECS)	BETA(DEG)	VOL(CUFT)	RADIUS(FT)	FORCE(LBS)
0.451998	3.11067	143.852	2.18129	855.361

THETA(DEG)	VLT(FPS)	RW(FPS)	VCN(FPS)	OMEGA(RAD/SEC)
51.9244	167.084	3.55711	-1.09000	0.150909

TIME(SECS)	BETA(DEG)	VOL(CUFT)	RADIUS(FT)	FORCE(LBS)
0.501997	3.42306	172.196	2.39203	1009.81

THETA(DEG)	VLT(FPS)	RW(FPS)	VCN(FPS)	OMEGA(RAD/SEC)
52.3655	162.835	4.40571	-1.56644	0.156301

TIME(SECS)	BETA(DEG)	VOL(CUFT)	RADIUS(FT)	FORCE(LBS)
0.551996	3.81237	210.422	2.65241	1194.91

THETA(DEG)	VLT(FPS)	RW(FPS)	VCN(FPS)	OMEGA(RAD/SEC)
52.8153	157.629	5.31289	-1.91017	0.157011

TIME(SECS)	BETA(DEG)	VOL(CUFT)	RADIUS(FT)	FORCE(LBS)
0.601996	4.29595	261.971	2.97193	1409.94

THETA(DEG)	VLT(FPS)	RW(FPS)	VCN(FPS)	OMEGA(RAD/SEC)
53.2616	151.293	6.20537	-2.10428	0.153996

TIME(SECS)	BETA(DEG)	VOL(CUFT)	RADIUS(FT)	FORCE(LBS)
0.651995	4.89744	331.512	3.36247	1650.95

THETA(DEG)	VLT(FPS)	RW(FPS)	VCN(FPS)	OMEGA(RAD/SEC)
53.6957	143.667	6.97251	-2.15939	0.148757

TIME(SECS)	BETA(DEG)	VOL(CUFT)	RADIUS(FT)	FORCE(LBS)
0.701995	5.65181	425.468	3.84009	1910.76
THETA(DEG)	VLT(FPS)	RW(FPS)	VCN(FPS)	OMEGA(RAD/SEC)
54.1137	134.622	7.47378	-2.10603	0.142974

TIME(SECS)	BETA(DEG)	VOL(CUFT)	RADIUS(FT)	FORCE(LBS)
0.751994	6.61641	552.986	4.42906	2180.92
THETA(DEG)	VLT(FPS)	RW(FPS)	VCN(FPS)	OMEGA(RAD/SEC)
54.5161	124.076	7.55701	-1.98182	0.138108

TIME(SECS)	BETA(DEG)	VOL(CUFT)	RADIUS(FT)	FORCE(LBS)
0.801993	7.89872	728.038	5.17214	2458.30
THETA(DEG)	VLT(FPS)	RW(FPS)	VCN(FPS)	OMEGA(RAD/SEC)
54.9071	111.987	7.08338	-1.81905	0.135155

TIME(SECS)	BETA(DEG)	VOL(CUFT)	RADIUS(FT)	FORCE(LBS)
0.851993	9.75002	975.311	6.16577	2770.45
THETA(DEG)	VLT(FPS)	RW(FPS)	VCN(FPS)	OMEGA(RAD/SEC)
55.2928	98.2653	5.93602	-1.63515	0.134553

TIME(SECS)	BETA(DEG)	VOL(CUFT)	RADIUS(FT)	FORCE(LBS)
0.901992	12.2019	1262.00	7.35082	2826.11
THETA(DEG)	VLT(FPS)	RW(FPS)	VCN(FPS)	OMEGA(RAD/SEC)
55.6820	83.0413	0.275904	-1.51679	0.139136

END OF SECOND FILLING PHASE

BEGINNING OF TRANSITION PHASE

STEADY STATE CANOPY VOLUME EQUALS 1292.47CU FT
STEADY STATE CANOPY RADIUS EQUALS 7.48724FT
HST EQUALS 0.829277FT. AND BETAST EQUALS 0.218339RADS

FINAL PHASE II RW EQUALS -1.55267FPS
INITIAL VALUE FOR RW FOR TRANS. PHASE EQ 3.33678FPS

TIME(SECS)	BETA(DEG)	FORCE(LBS)	VLT(FPS)	LENGTH(FT)
1.01099	13.0902	976.350	55.4796	31.4806
THETA(DEG)	RW(FPS)	VCN(FPS)	OMEGA(RD/SEC)	
56.6914	-23.5077	-2.10969	0.190587	

TIME(SECS)	BETA(DEG)	FORCE(LBS)	VLT(FPS)	LENGTH(FT)
1.11000	14.0052	122.299	48.9713	29.4611
THETA(DEG)	RW(FPS)	VCN(FPS)	OMEGA(RD/SEC)	
57.9422	-15.8475	-2.82439	0.250439	

TIME(SECS)	BETA(DEG)	FORCE(LBS)	VLT(FPS)	LENGTH(FT)
1.21000	14.4675	42.6589	47.8726	28.5388
THETA(DEG)	RW(FPS)	VCN(FPS)	OMEGA(RD/SEC)	
59.5186	-3.76408	-3.52420	0.296657	

TIME(SECS)	BETA(DEG)	FORCE(LBS)	VLT(FPS)	LENGTH(FT)
1.31001	14.4890	217.216	46.0274	28.4974
THETA(DEG)	RW(FPS)	VCN(FPS)	OMEGA(RD/SEC)	
61.3012	1.73288	-4.12543	0.323326	

TIME(SECS)	BETA(DEG)	FORCE(LBS)	VLT(FPS)	LENGTH(FT)
1.41001	14.3900	321.982	42.8341	28.6893
THETA(DEG)	RW(FPS)	VCN(FPS)	OMEGA(RD/SEC)	
63.2045	1.66064	-4.64702	0.340446	

TIME(SECS)	BETA(DEG)	FORCE(LBS)	VLT(FPS)	LENGTH(FT)
1.51001	14.3461	314.612	39.6048	28.7752
THETA(DEG)	RW(FPS)	VCN(FPS)	OMEGA(RD/SEC)	
65.1974	0.121788	-5.12113	0.355167	

TIME(SECS)	BETA(DEG)	FORCE(LBS)	VLT(FPS)	LENGTH(FT)
1.61002	14.3632	268.510	37.1501	28.7417
THETA(DEG)	RW(FPS)	VCN(FPS)	OMEGA(RD/SEC)	
67.2703	-0.638844	-5.55814	0.368046	

TIME(SECS)	BETA(DEG)	FORCE(LBS)	VLT(FPS)	LENGTH(FT)
1.71002	14.3948	237.452	35.4439	28.6800
THETA(DEG)	RW(FPS)	VCN(FPS)	OMEGA(RD/SEC)	
69.4071	-0.543065	-5.95372	0.377165	

TIME(SECS)	BETA(DEG)	FORCE(LBS)	VLT(FPS)	LENGTH(FT)
1.81003	14.4137	228.468	34.1564	28.6432
THETA(DEG)	RW(FPS)	VCN(FPS)	OMEGA(RD/SEC)	
71.5823	-0.220812	-6.30131	0.381293	

TIME(SECS)	BETA(DEG)	FORCE(LBS)	VLT(FPS)	LENGTH(FT)
1.91003	14.4195	228.304	33.0598	28.6317
THETA(DEG)	RW(FPS)	VCN(FPS)	OMEGA(RD/SEC)	
73.7668	-4.75531E-02	-6.59731	0.380441	

TIME(SECS)	BETA(DEG)	FORCE(LBS)	VLT(FPS)	LENGTH(FT)
2.01004	14.4212	226.931	32.0906	28.6286
THETA(DEG)	RW(FPS)	VCN(FPS)	OMEGA(RD/SEC)	
75.9335	-3.62383E-02	-6.84028	0.375116	

TIME(SECS)	BETA(DEG)	FORCE(LBS)	VLT(FPS)	LENGTH(FT)
2.11003	14.4239	222.614	31.2553	28.6233
THETA(DEG)	RW(FPS)	VCN(FPS)	OMEGA(RD/SEC)	
78.0580	-7.37384E-02	-7.02922	0.365730	

BREAK IN PRINYOUT HERE TO SAVE SPACE

TIME(SECS)	BETA(DEG)	FORCE(LBS)	VLT(FPS)	LENGTH(FT)
2.91097	14.4518	193.173	27.8949	28.5692
THETA(DEG)	RW(FPS)	VCN(FPS)	OMEGA(RD/SEC)	
91.1987	-5.22438E-02	-6.55442	0.181046	

TIME(SECS)	BETA(DEG)	FORCE(LBS)	VLT(FPS)	LENGTH(FT)
3.01096	14.4543	190.705	27.7164	28.5644
THETA(DEG)	RW(FPS)	VCN(FPS)	OMEGA(RD/SEC)	
92.1497	-4.64431E-02	-6.26577	0.150566	

TIME(SECS)	BETA(DEG)	FORCE(LBS)	VLT(FPS)	LENGTH(FT)
3.11096	14.4564	188.582	27.5726	28.5602
THETA(DEG)	RW(FPS)	VCN(FPS)	OMEGA(RD/SEC)	
92.9256	-4.02695E-02	-5.93584	0.119985	

TIME(SECS)	BETA(DEG)	FORCE(LBS)	VLT(FPS)	LENGTH(FT)
3.21095	14.4583	186.808	27.4599	28.5566
THETA(DEG)	RW(FPS)	VCN(FPS)	OMEGA(RD/SEC)	
93.5271	-3.38517E-02	-5.56892	8.97552E-02	

TIME(SECS)	BETA(DEG)	FORCE(LBS)	VLT(FPS)	LENGTH(FT)
3.31094	14.4598	185.387	27.3752	28.5537
THETA(DEG)	RW(FPS)	VCN(FPS)	OMEGA(RD/SEC)	
93.9573	-2.72760E-02	-5.16971	6.03079E-02	

TIME(SECS)	BETA(DEG)	FORCE(LBS)	VLT(FPS)	LENGTH(FT)
3.41094	14.4610	184.320	27.3150	28.5513
THETA(DEG)	RW(FPS)	VCN(FPS)	OMEGA(RD/SEC)	
94.2220	-2.07229E-02	-4.74327	3.20465E-02	

TIME(SECS)	BETA(DEG)	FORCE(LBS)	VLT(FPS)	LENGTH(FT)
3.51093	14.4619	183.587	27.2762	28.5496
THETA(DEG)	RW(FPS)	VCN(FPS)	OMEGA(RD/SEC)	
94.3291	-1.44942E-02	-4.29498	5.34339E-03	

TIME(SECS)	BETA(DEG)	FORCE(LBS)	VLT(FPS)	LENGTH(FT)
3.61092	14.4625	183.153	27.2552	28.5485
THETA(DEG)	RW(FPS)	VCN(FPS)	OMEGA(RD/SEC)	
94.2884	-8.89619E-03	-3.83049	-1.94656E-02	

TIME(SECS)	BETA(DEG)	FORCE(LBS)	VLT(FPS)	LENGTH(FT)
3.71091	14.4628	182.989	27.2486	28.5479
THETA(DEG)	RW(FPS)	VCN(FPS)	OMEGA(RD/SEC)	
94.1116	-4.01141E-03	-3.35568	-4.20845E-02	

TIME(SECS)	BETA(DEG)	FORCE(LBS)	VLT(FPS)	LENGTH(FT)
3.81091	14.4629	183.026	27.2532	28.5477
THETA(DEG)	RW(FPS)	VCN(FPS)	OMEGA(RD/SEC)	
93.8120	-8.20918E-05	-2.87656	-6.22611E-02	

TIME(SECS)	BETA(DEG)	FORCE(LBS)	VLT(FPS)	LENGTH(FT)
3.91090	14.4628	183.219	27.2657	28.5479
THETA(DEG)	RW(FPS)	VCN(FPS)	OMEGA(RD/SEC)	
93.4043	2.92303E-03	-2.39922	-7.97895E-02	

TIME(SECS)	BETA(DEG)	FORCE(LBS)	VLT(FPS)	LENGTH(FT)
4.01089	14.4627	183.474	27.2831	28.5482

```
THETA(DEG)        RW(FPS)         VCN(FPS)         OMEGA(RD/SEC)
    92.9040     4.92302E-03    -1.92973    -9.45134E-02


TIME(SECS)          BETA(DEG)        FORCE(LBS)     VLT(FPS)    LENGTH(FT)
    4.11088     14.4623     183.860     27.3025     28.5488
THETA(DEG)        RW(FPS)         VCN(FPS)         OMEGA(RD/SEC)
    92.3277     5.84737E-03    -1.47400   -0.106327


TIME(SECS)          BETA(DEG)        FORCE(LBS)     VLT(FPS)    LENGTH(FT)
    4.21088     14.4620     184.205     27.3214     28.5495
THETA(DEG)        RW(FPS)         VCN(FPS)         OMEGA(RD/SEC)
    91.6919     5.22327E-03    -1.03772   -0.115176


TIME(SECS)          BETA(DEG)        FORCE(LBS)     VLT(FPS)    LENGTH(FT)
    4.31087     14.4618     184.417     27.3387     28.5499
THETA(DEG)        RW(FPS)         VCN(FPS)         OMEGA(RD/SEC)
    91.0139     5.14782E-03   -0.626208   -0.121060


TIME(SECS)          BETA(DEG)        FORCE(LBS)     VLT(FPS)    LENGTH(FT)
    4.41086     14.4616     184.654     27.3526     28.5503
THETA(DEG)        RW(FPS)         VCN(FPS)         OMEGA(RD/SEC)
    90.3105     4.81418E-03   -0.244295   -0.124025


TIME(SECS)          BETA(DEG)        FORCE(LBS)     VLT(FPS)    LENGTH(FT)
    4.51086     14.4614     184.813     27.3620     28.5506
THETA(DEG)        RW(FPS)         VCN(FPS)         OMEGA(RD/SEC)
    89.5982     4.09617E-03     1.03768E-01   -0.124171


TIME(SECS)          BETA(DEG)        FORCE(LBS)     VLT(FPS)    LENGTH(FT)
    4.61085     14.4612     184.918     27.3660     28.5510
THETA(DEG)        RW(FPS)         VCN(FPS)         OMEGA(RD/SEC)
    88.8926     1.88966E-03    0.414419   -0.121641


TIME(SECS)          BETA(DEG)        FORCE(LBS)     VLT(FPS)    LENGTH(FT)
    4.71084     14.4612     184.835     27.3649     28.5510
THETA(DEG)        RW(FPS)         VCN(FPS)         OMEGA(RD/SEC)
    88.2088    -7.62786E-04    0.684843   -0.116623
```

TIME(SECS)	BETA(DEG)	FORCE(LBS)	VLT(FPS)	LENGTH(FT)
4.81083	14.4613	184.645	27.3594	28.5508
THETA(DEG)	RW(FPS)	VCN(FPS)	OMEGA(RD/SEC)	
87.5602	-2.82502E-03	0.913006	-0.109339	

TIME(SECS)	BETA(DEG)	FORCE(LBS)	VLT(FPS)	LENGTH(FT)
4.91083	14.4615	184.424	27.3504	28.5504
THETA(DEG)	RW(FPS)	VCN(FPS)	OMEGA(RD/SEC)	
86.9592	-3.85151E-03	1.09768	-1.00042E-01	

TIME(SECS)	BETA(DEG)	FORCE(LBS)	VLT(FPS)	LENGTH(FT)
5.01082	14.4617	184.164	27.3382	28.5501
THETA(DEG)	RW(FPS)	VCN(FPS)	OMEGA(RD/SEC)	
86.4165	-5.31595E-03	1.23846	-8.90130E-02	

TIME(SECS)	BETA(DEG)	FORCE(LBS)	VLT(FPS)	LENGTH(FT)
5.11081	14.4620	183.792	27.3246	28.5494
THETA(DEG)	RW(FPS)	VCN(FPS)	OMEGA(RD/SEC)	
85.9412	-5.45431E-03	1.33571	-7.65486E-02	

TIME(SECS)	BETA(DEG)	FORCE(LBS)	VLT(FPS)	LENGTH(FT)
5.21080	14.4623	183.539	27.3102	28.5489
THETA(DEG)	RW(FPS)	VCN(FPS)	OMEGA(RD/SEC)	
85.5407	-5.11840E-03	1.39052	-6.29591E-02	

TIME(SECS)	BETA(DEG)	FORCE(LBS)	VLT(FPS)	LENGTH(FT)
5.31080	14.4626	183.222	27.2959	28.5484
THETA(DEG)	RW(FPS)	VCN(FPS)	OMEGA(RD/SEC)	
85.2205	-5.00715E-03	1.40468	-4.85611E-02	

TIME(SECS)	BETA(DEG)	FORCE(LBS)	VLT(FPS)	LENGTH(FT)
5.41079	14.4628	182.973	27.2826	28.5479
THETA(DEG)	RW(FPS)	VCN(FPS)	OMEGA(RD/SEC)	
84.9844	-5.01031E-03	1.38058	-3.36704E-02	

TIME(SECS)	BETA(DEG)	FORCE(LBS)	VLT(FPS)	LENGTH(FT)
5.51078	14.4630	182.775	27.2709	28.5476
THETA(DEG)	RW(FPS)	VCN(FPS)	OMEGA(RD/SEC)	
84.8342	-5.08950E-03	1.32112	-1.85966E-02	

TIME(SECS)	BETA(DEG)	FORCE(LBS)	VLT(FPS)	LENGTH(FT)
5.61078	14.4632	182.611	27.2619	28.5472
THETA(DEG)	RW(FPS)	VCN(FPS)	OMEGA(RD/SEC)	
84.7702	-4.51721E-03	1.22970	-3.63787E-03	

TIME(SECS)	BETA(DEG)	FORCE(LBS)	VLT(FPS)	LENGTH(FT)
5.71077	14.4633	182.489	27.2561	28.5469
THETA(DEG)	RW(FPS)	VCN(FPS)	OMEGA(RD/SEC)	
84.7909	-2.80738E-03	1.11005	1.09237E-02	

TIME(SECS)	BETA(DEG)	FORCE(LBS)	VLT(FPS)	LENGTH(FT)
5.81076	14.4634	182.502	27.2535	28.5468
THETA(DEG)	RW(FPS)	VCN(FPS)	OMEGA(RD/SEC)	
84.8933	-3.17685E-04	0.966224	2.48261E-02	

TIME(SECS)	BETA(DEG)	FORCE(LBS)	VLT(FPS)	LENGTH(FT)
5.91075	14.4634	182.561	27.2533	28.5468
THETA(DEG)	RW(FPS)	VCN(FPS)	OMEGA(RD/SEC)	
85.0729	1.33544E-03	0.802478	3.78316E-02	